

Part-I: model
description, sea salt
aerosols and pH

A. Kerkweg et al.

Consistent simulation of bromine chemistry from the marine boundary layer to the stratosphere, Part I: model description, sea salt aerosols and pH

A. Kerkweg^{1,2}, P. Jöckel¹, A. Pozzer¹, H. Tost¹, R. Sander¹, M. Schulz³, P. Stier⁴, E. Vignati⁵, J. Wilson⁵, and J. Lelieveld¹

¹Atmospheric Chemistry Department, Max Planck Institute of Chemistry, P.O. Box 3060, 55020 Mainz, Germany

²Institute for Atmospheric Physics, University of Mainz, Germany

³Laboratoire des Sciences du Climat et de l'Environnement, CEA-IPSL, Saclay, France

⁴Atmospheric, Oceanic and Planetary Physics, University of Oxford, UK

⁵Joint Research Centre, Institute of Environment and Sustainability, Ispra, Italy

Received: 26 February 2008 – Accepted: 10 March 2008 – Published: 14 April 2008

Correspondence to: A. Kerkweg (akerkweg@mpch-mainz.mpg.de)

Published by Copernicus Publications on behalf of the European Geosciences Union.

Title Page

Abstract

Introduction

Conclusions

References

Tables

Figures

◀

▶

◀

▶

Back

Close

Full Screen / Esc

Printer-friendly Version

Interactive Discussion



Abstract

This is the first article of a series presenting a detailed analysis of bromine chemistry simulated with the atmospheric chemistry general circulation model ECHAM5/MESSy. Release from sea salt is an important bromine source, hence the model explicitly calculates aerosol chemistry and phase partitioning for coarse mode aerosol particles. Many processes including chemical reaction rates are influenced by the particle size distribution, and aerosol associated water strongly affects the aerosol pH. Knowledge of the aerosol pH is important as it determines the aerosol chemistry, e.g., the efficiency of sulphur oxidation and bromine release. Here, we focus on the simulated sea salt aerosol size distribution and the coarse mode aerosol pH.

A comparison with available field data shows that the simulated aerosol distributions agree reasonably well within the range of measurements. In spite of the small number of aerosol pH measurements and the uncertainty in its experimental determination, the simulated aerosol pH compares well with the observations. The aerosol pH ranges from alkaline aerosol in areas of strong production down to pH values of 1 over regions of medium sea salt production and high levels of gas phase acids, mostly polluted regions over the oceans in the northern hemisphere.

1 Introduction

Halogen containing compounds that photochemically decompose in the stratosphere contribute to catalytic ozone destruction. Reactive bromine is less easily deactivated into reservoir species compared to chlorine, hence its ozone destroying efficiency is about 50 times higher (Brasseur and Solomon, 2005). Though less dramatic, similar processes have been shown to occur in the marine boundary layer, as indicated by the depletion of chlorine and bromine in sea salt aerosol particles (Sander et al., 2003). In contrast to prior model studies investigating only one of these two phenomena/domains, the model simulation discussed here is dedicated to consistently

Part-I: model description, sea salt aerosols and pH

A. Kerkweg et al.

Title Page

Abstract

Introduction

Conclusions

References

Tables

Figures

◀

▶

◀

▶

Back

Close

Full Screen / Esc

Printer-friendly Version

Interactive Discussion



**Part-I: model
description, sea salt
aerosols and pH**

A. Kerkweg et al.

Title Page

Abstract

Introduction

Conclusions

References

Tables

Figures

◀

▶

◀

▶

Back

Close

Full Screen / Esc

Printer-friendly Version

Interactive Discussion



simulate bromine chemistry from the boundary layer to the stratosphere. We used the atmospheric chemistry general circulation model (AC-GCM) ECHAM5/MESSy (<http://www.messy-interface.org>), because this model is able to consistently simulate chemistry in this entire domain (Jöckel et al., 2006). For a list of abbreviations, see Table 1. One aim of this work is to compute both column integrated and vertically resolved reactive bromine (e.g. BrO) concentrations that can be directly compared to global satellite measurements (Wagner et al., 2001). The latter will be pursued in a follow-up article, whereas here we focus on the marine boundary layer.

One important bromine source is sea salt aerosol. Therefore, an adequate aerosol representation must be available in the model, on which we focus in the present article. In recent years much progress has been made in incorporating aerosols into global models (Lauer et al., 2005; Stier et al., 2005; Gong et al., 2003; Spracklen et al., 2005), following the overall tendency in atmospheric modelling to include additional details of processes. Most of these models focus on aerosol microphysical processes, and neglect or simplify aerosol chemistry. E.g. Stier et al. (2005) included only the phase transition of sulphate, i.e. the condensation of gas phase acids onto aerosol modes/bins; Lauer et al. (2005) used thermodynamic equilibrium chemistry. In this simulation gas and aerosol phase chemistry is calculated in great detail (Kerkweg et al., 2007). We prognostically calculate the chemistry in the aerosol phase, i.e. without equilibrium assumptions using an explicit aqueous phase mechanism for the reactions in the coarse mode aerosol, the heterogeneous reactions on the coarse mode and the phase transition reactions. To our knowledge, this is the first global simulation attempting this in such detail. One of the advantages of this approach is that the H^+ concentration is included like other chemical species, which allows a prognostic calculation of the aerosol pH.

The chemistry releasing bromine from the aerosol is strongly pH dependent, as bromine is efficiently released from acidified aerosol ($pH < 5.5$) only. In fact, all aerosol chemistry depends on the aerosol pH. In turn, the pH is influenced by the size distribution and the liquid water content of the aerosol particles (von Glasow and Sander,

2001). Since the sea salt aerosol mass is dominated by the coarse size fraction the particle distribution and the aerosol pH for coarse mode aerosol are evaluated here.

Section 2 gives a description of the model used for this study with a special focus on the aerosol dynamical model (Sect. 2.4) and the aerosol chemistry model (Sect. 2.5).

5 In Sect. 3 we provide an overview of the simulated aerosol distributions (Sect. 3.1) and discuss the simulated aerosol pH values (Sect. 3.2) before we draw our conclusions (Sect. 4).

2 Model description

For this study we used the atmospheric chemistry general circulation model (AC-GCM) ECHAM5/MESSy1 (E5/M1). ECHAM5 is the 5th generation European Centre Ham-
10 burg GCM (Roeckner et al., 2003, 2004). It is coupled to the Modular Earth Submodel System (MESSy) (Jöckel et al., 2005) which includes atmospheric chemistry and dynamics related submodels. The coupled E5/M1 model has been extensively evaluated by Jöckel et al. (2006).

15 To adapt the model to the needs of this study we introduced one important change. Since one of the main foci of the present simulation is bromine chemistry in the marine boundary layer and in the free troposphere, a model providing a higher resolution of the lower part of the atmosphere is desirable. For this, we applied a vertical resolution with 87 layers (L87) on a hybrid-pressure grid reaching from the surface
20 up to 0.01 hPa (≈ 80 km altitude) as available in the ECHAM5 version 5.3.02. This resolution divides the boundary layer into more vertical layers than the L90 version (used in the evaluation of Jöckel et al. (2006)). While the L87 version has a much better resolution in the lowest part of the atmosphere, the resolution of the L90 version is better in the upper troposphere and stratosphere. A figure illustrating this can
25 be found in the supplement (<http://www.atmos-chem-phys-discuss.net/8/7217/2008/acpd-8-7217-2008-supplement.zip>). Referring to the physical description the changed MESSy version (M1⁺), used for this study, is basically the same as MESSy version 1

Part-I: model description, sea salt aerosols and pH

A. Kerkweg et al.

Title Page

Abstract

Introduction

Conclusions

References

Tables

Figures

◀

▶

◀

▶

Back

Close

Full Screen / Esc

Printer-friendly Version

Interactive Discussion



(M1) described and evaluated in [Jöckel et al. \(2006\)](#).

2.1 Model setup

We discuss two simulations in this paper. First we repeated the evaluation simulation of [Jöckel et al. \(2006\)](#) to show that the model in the L87 vertical resolution setup produces comparable results to the L90 setup used by [Jöckel et al. \(2006\)](#). In the following this simulation is referred to as S-new. It was performed for the years 1998–2000. The second simulation will be denoted as S-hal simulation. It is the main simulation discussed in this series of articles, and it comprises explicit aerosol and bromine chemistry calculations. S-hal covers the period of January 1998 to December 2000. The first two years are used as model spin up (especially needed to ensure that the aerosol distribution and the aerosol chemistry are in dynamic equilibrium), and the year 2000 is analysed here.

The resolution is T42L87MA (MA stands for Middle Atmosphere, see [Giorgetta et al.; Giorgetta et al., 2002; 2006](#)). The horizontal resolution (T42) corresponds to a quadratic Gaussian grid of approximately $2.8^\circ \times 2.8^\circ$ (same as used by [Jöckel et al., 2006](#)) in longitude and latitude. The model timestep is 720 s. To capture diurnal cycles, results are sampled as 5-hourly instantaneous output for almost all fields. This enables us to resolve an hourly diurnal cycle every 5 days of simulation.

[Jöckel et al. \(2006\)](#) and [Giorgetta et al. \(2006\)](#) showed that MA-ECHAM5 is able to produce a selfconsistent Quasi-Biennial Oscillation (QBO). Since we are in the present study not primarily interested in showing that the QBO is developing in the model by itself, it was forced by the MESSy submodel QBO to yield the observed QBO phase.

In addition, temperature, vorticity, divergence and the logarithm of the surface pressure of the model have been nudged towards the analysis data from the European Centre of Medium-range Weather Forecasts (ECMWF) operational weather forecast model to represent the observed meteorology in the troposphere ([Jeuken et al., 1996; Jöckel et al., 2006](#)). The nudging was applied from above the boundary layer up to 200 hPa, thus the stratosphere as well as the boundary layer are calculated freely.

Part-I: model description, sea salt aerosols and pH

A. Kerkweg et al.

Title Page

Abstract

Introduction

Conclusions

References

Tables

Figures

◀

▶

◀

▶

Back

Close

Full Screen / Esc

Printer-friendly Version

Interactive Discussion



**Part-I: model
description, sea salt
aerosols and pH**

A. Kerkweg et al.

Title Page

Abstract

Introduction

Conclusions

References

Tables

Figures

◀

▶

◀

▶

Back

Close

Full Screen / Esc

Printer-friendly Version

Interactive Discussion



Most emissions are calculated from monthly offline fields using the submodel OF-FLEM (Kerkweg et al., 2006b). For a detailed description of all submodels mentioned here see Jöckel et al. (2006). A list of annually integrated emission fluxes of most trace gases can be found in the supplement of Pozzer et al. (2007). To calculate online emissions for oceanic DMS (dimethyl sulphide), NO, isoprene and aerosols the MESSy submodel ONLEM (Kerkweg et al., 2006b) is used. The aerosol emissions are further described in the section about the aerosol model M7 (Sect. 2.4). 4.2 Tg NO_x per year are produced by lightning (submodel LNOX, Tost et al. (2007)).

For some trace gases the emission fluxes are highly uncertain, while the atmospheric concentrations in the boundary layer are relatively well known. Thus the mixing ratios of N₂O, CH₄, CFCl₃, CH₃CCl₃, CCl₄, CF₂ClBr, CF₃Br, H₂, CO₂, SF₆, CH₃Cl and CH₃Br are nudged towards the observed values in the lowest model layer using the submodel TNUDGE (Kerkweg et al., 2006b). To improve the emissions of acetone and methanol from the ocean (Pozzer et al., 2007), the submodel AIRSEA is used (Pozzer et al., 2006).

Dry deposition of gas phase species and aerosol particles and sedimentation of aerosol particles are calculated via the MESSy submodels DRYDEP and SEDI, respectively (Kerkweg et al., 2006a).

Cloud formation is calculated via the submodels CLOUD and CONVECT (Tost et al., 2006b, 2007). Convective transport of trace gases and aerosol particles is included via the submodel CVTRANS. Scavenging, cloud chemistry and wet deposition are calculated by SCAV (Tost et al., 2006a). Gas and aerosol phase chemistry are simulated by MECCA(-AERO) (Sander et al., 2005; Kerkweg et al., 2007). Photolysis rates required by MECCA are calculated with the submodel JVAL following the approach of Landgraf and Crutzen (1998). The submodel H2O feeds back the effect of the methane oxidation to the specific humidity. Heterogeneous reaction rates and the partitioning of total water into water vapour, liquid water and ice for polar stratospheric clouds (PSCs) as well as outside the PSC region, are accounted for in the submodels PSC and HETCHEM, respectively. Aerosol microphysics is calculated using the submodel M7 (see Sect. 2.4).

The temperature tendencies due to radiative heating (submodel RAD4ALL) are calculated by using the online-calculated mixing ratios of CO₂, N₂O, CFCI₃, CF₂Cl₂, cloud cover, water vapour, cloud water content, and cloud ice. For the aerosol radiative effects the same aerosol climatology is used as in [Jöckel et al. \(2006\)](#).

In addition to the submodels listed above, we included several diagnostic submodels. The only one important for the present analysis is TROPOP which diagnoses the tropopause and the boundary layer height.

2.2 Hardware

All simulations were performed on the IBM pSeries “Regatta” system based on Power 4 processor technology at the Max Planck “computer center Garching”. We used 256 CPUs (8 compute nodes). One month simulation time of the reference simulation required a wall-clock time of approximately 14 hours. The most demanding process is the aerosol chemistry, a sensitivity simulation not including the explicit aerosol chemistry only required half of the CPU time of the reference simulation.

2.3 Comparison to the evaluated model results

Because some important changes have been applied between the model setup used by [Jöckel et al. \(2006\)](#) and the model setup discussed here, a comparison of the results obtained by both model configurations with the same setup is required. Thus a simulation (S-new), with the setup as described by [Jöckel et al. \(2006\)](#) for the S2 simulation, i.e. using the same submodels and namelist settings, was performed. The main difference is the model resolution (T42L87MA versus T42L90MA) and the application of some additional diagnostic tools. Overall the results of both simulations agree well within the expected uncertainties. The electronic supplement (<http://www.atmos-chem-phys-discuss.net/8/7217/2008/acpd-8-7217-2008-supplement.zip>) includes almost all figures corresponding to those in [Jöckel et al. \(2006\)](#).

Part-I: model description, sea salt aerosols and pH

A. Kerkweg et al.

Title Page

Abstract

Introduction

Conclusions

References

Tables

Figures

◀

▶

◀

▶

Back

Close

Full Screen / Esc

Printer-friendly Version

Interactive Discussion



2.4 The microphysical aerosol model M7

A major source of bromine in the atmosphere is the release from sea salt. Kerkweg et al. (2007) describe the submodel MECCA-AERO calculating the release via an explicit gas and aerosol phase chemistry mechanism. One important input parameter for these calculations is the aerosol distribution, which is required by MECCA-AERO, and computed by an aerosol dynamical model (ADM). The ADM M7 (Vignati et al., 2004), which describes the aerosol distribution by 7 log-normal modes (4 soluble, 3 insoluble), was implemented as a submodel into the MESSy system. The box-model M7 was developed and is used by Stier et al. (2005) in ECHAM5-HAM. Emissions and loss processes of particles are not part of M7, but are calculated by other MESSy submodels (e.g. ONLEM, DRYDEP and SCAV). Thus we are using the same microphysical core as Stier et al. (2005), but source and sink processes are implemented differently. For example, H_2SO_4 is determined by the full chemical reaction mechanism as given by MECCA(-AERO), whereas Stier et al. (2005) calculates H_2SO_4 by the oxidation of DMS and SO_2 by prescribed OH.

M7 distinguishes five different aerosol components: sulphate (SU), black carbon (BC), soluble and insoluble organic carbon (OC), sea salt (SS) and dust (DU). It distributes aerosol masses and particle numbers into 7 log-normal modes. Three of these modes contain only insoluble material (BC, OC and DU) and four modes are assumed to be internally mixed containing soluble material (SU, OC and SS). Insoluble particles can be coated by sulphate, thus becoming soluble particles. Consequently, the larger soluble modes can contain all five components. Table 2 summarises the distribution of the different components among the modes and lists the corresponding dry radius ranges for the modes. The total particle number as well as the masses of the components of each mode are calculated prognostically, whereas the mean dry radius and the mean ambient radius are determined diagnostically. The radius standard deviation for each mode is kept constant ($\sigma=2.0$ for the coarse modes and $\sigma=1.59$ for the other modes).

Part-I: model description, sea salt aerosols and pH

A. Kerkweg et al.

Title Page

Abstract

Introduction

Conclusions

References

Tables

Figures

◀

▶

◀

▶

Back

Close

Full Screen / Esc

Printer-friendly Version

Interactive Discussion



This modal structure requires 18 mass tracers and 7 number tracers, i.e. 25 aerosol tracers in total.

M7 simulates the following processes:

- Nucleation of sulphate particles, for which the mechanism by [Vehkamäki et al. \(2002\)](#) is applied.
- Condensation of H_2SO_4 onto all modes enabling the transfer of insoluble particle mass into soluble modes.
- Coagulation of aerosols.
- Transition from smaller to larger modes.

More details about the individual processes as simulated by M7 are given in [Wilson et al. \(2001\)](#), [Vignati et al. \(2004\)](#) and [Stier et al. \(2005\)](#).

2.4.1 Emissions

Sea salt emissions are particularly important for the release of reactive bromine in the marine boundary layer. The scheme used for our simulation applies lookup tables. It is a wind speed dependent interpolation between the emission functions of [Mona-](#)
[han \(1986\)](#) and [Smith and Harrison \(1998\)](#). Since they depend on the aerosol mode definition, the lookup tables are especially designed for M7 emissions ([Guelle et al., 2001](#); [Schulz et al., 2004](#)). Table 3 lists the annual primary emission fluxes for all M7 components. Primary emissions of sulphate are not taken into account in this model study. Furthermore, the budget of sulphate is rather low as we did not include volcanic emissions in our emission inventory, i.e. $\approx 12\text{Tg(S)}/\text{yr}$ are missing. The organic and black carbon emissions used in this study have been adopted from the AeroCom B experiment ([Dentener et al. \(2006\)](#), <http://nansen.ipsl.jussieu.fr/AEROCOM/>). They are subdivided into fossil fuel, biogenic fuel, wildfire emissions and Secondary Organic Aerosol (SOA) formation. The mineral dust emissions depend on the soil moisture, a source strength factor, a threshold velocity and the clay fraction of the uppermost

**Part-I: model
description, sea salt
aerosols and pH**

A. Kerkweg et al.

Title Page

Abstract

Introduction

Conclusions

References

Tables

Figures

◀

▶

◀

▶

Back

Close

Full Screen / Esc

Printer-friendly Version

Interactive Discussion



soil layer (Balkanski et al., 2003). A more detailed description of all online calculated sources can be found in Kerkweg et al. (2006b).

2.4.2 Dry deposition of aerosol particles

The deposition velocity of each aerosol mode is calculated according to the big leaf approach depending on six different surface types, the mean radius and the radius standard deviation of the aerosol mode (Wesely, 1989; Ganzeveld and Lelieveld, 1995). A detailed description of the dry deposition algorithm of the MESSy submodel DRYDEP is given in Kerkweg et al. (2006a).

2.4.3 Sedimentation of aerosol particles

Sedimentation is calculated by the submodel SEDI (Kerkweg et al., 2006a). It is based on the theory of aerosol sedimentation (see for example Pruppacher and Klett, 1997). The terminal velocity is determined for each individual mode depending on the aerosol density, ambient radius and the standard deviation. This velocity is corrected for aerodynamic differences between ideal spheres and real non-spherical particles by the Cunningham-slip-flow factor. In addition, for lognormal distributions the particle radius varies over a wider range and the mean sedimentation velocity of all particles of a lognormal mode is larger than the sedimentation velocity for a particle of the mean radius. Therefore, a correction factor – the so-called Slinn factor – is applied (Slinn and Slinn, 1980).

2.4.4 Scavenging and wet removal of aerosol particles

A very important sink of trace gases and aerosols is scavenging and subsequent wet deposition. The SCAV submodel (Tost et al., 2006a) simulates large scale and convective scavenging in rain, snow and ice, accounting for nucleation and impaction scavenging. Note: the scavenging and cloud processes do not include an online-calculated

Part-I: model description, sea salt aerosols and pH

A. Kerkweg et al.

Title Page

Abstract

Introduction

Conclusions

References

Tables

Figures

◀

▶

◀

▶

Back

Close

Full Screen / Esc

Printer-friendly Version

Interactive Discussion



activation of the aerosol. The cloud droplet number is still determined as in the standard ECHAM5 (i.e. a number is used, constant in time but pressure dependent, which is calculated at the beginning of the simulation).

The scavenging of aerosols is calculated using a size dependent coagulation/coalescence kernel. Thus a scavenging rate for each mode of an aerosol model is computed and assigned to the respective aerosol component tracers of this mode. Consequently, in case of M7 all components of the seven modes are subject to impaction scavenging and subsequent cloud processing. The wet deposition flux of the aerosol component results from the concentration of each species in the precipitation.

In addition, aerosol and cloud chemistry are explicitly coupled. The individual aerosol components (e.g. sulphate) are transferred to the droplets when the aerosol is scavenged. When droplets evaporate, volatile components are released into the gas phase, whereas the others become aerosol components of the largest available aerosol mode (which is the coarse mode in the present study).

In case of the explicit calculation of aerosol chemistry parallel to the aerosol dynamical model cloud chemistry is calculated for the coarse mode species defined by the aerosol chemistry model. The details about this cloud-aerosol chemistry coupling are discussed in detail in [Kerkweg et al. \(2007\)](#).

2.5 The aerosol chemistry model

In our model aerosol chemistry is explicitly calculated using the MESSy submodel MECCA-AERO ([Kerkweg et al., 2007](#)). MECCA-AERO uses the Kinetic PreProcessor (KPP, [Damian et al.](#); [Sandu and Sander, 2002; 2006](#)) to solve the differential equation set of the reaction mechanism. The reaction mechanism comprises 146 species reacting in 191 gas phase reactions, 65 photolysis reactions, and 10 heterogeneous reactions on polar stratospheric clouds. In the aqueous phase 13 acid-base equilibria, 24 phase transitions and 14 redox reactions are taken into account. In the supplement a complete list of all reactions included in the simulation is given. All reactions and equilibria are explicitly calculated, hence the aerosol pH is also prognostically deter-

Part-I: model description, sea salt aerosols and pH

A. Kerkweg et al.

Title Page

Abstract

Introduction

Conclusions

References

Tables

Figures

◀

▶

◀

▶

Back

Close

Full Screen / Esc

Printer-friendly Version

Interactive Discussion



**Part-I: model
description, sea salt
aerosols and pH**

A. Kerkweg et al.

[Title Page](#)[Abstract](#)[Introduction](#)[Conclusions](#)[References](#)[Tables](#)[Figures](#)[⏪](#)[⏩](#)[◀](#)[▶](#)[Back](#)[Close](#)[Full Screen / Esc](#)[Printer-friendly Version](#)[Interactive Discussion](#)

mined in this simulation. The H^+ concentration is treated like all other aerosol phase species concentrations, i.e. the pH is a direct result of the phase transitions and of the reactions in the aerosol phase. These themselves depend on the liquid water content (ambient radius), the abundance of the species in gas and aerosol phase and physical constants such as temperature, pressure etc. Details on the determination of the rate constants are given in [Kerkweg et al. \(2007\)](#).

MECCA-AERO is affected by numerical instabilities arising from the extreme stiffness of the kinetic ODE (ordinary differential equation) system (see discussion in [Kerkweg et al., 2007](#)). Consequently, for this study explicit aerosol chemistry was calculated for only one aerosol mode. Since coarse mode sea salt aerosol is the dominant source of bromine, the physical information about the coarse mode of the ADM M7 is used in the present simulation. The solver was only stable when aerosol chemistry was limited to aerosols with a liquid water content larger than $10^{-12} \text{ m}^3(\text{aq})/\text{m}^3(\text{air})$. In the marine boundary layer the coarse mode aerosol water content is usually larger than this threshold while it is smaller over land and in the free troposphere. Thus the source of bromine through aerosol chemistry is expected to be realistic, while the recycling of bromine on the accumulation mode is ignored. Additionally the heterogeneous reactions (e.g., HNO_3 uptake) are ignored in the free troposphere and over the continents where the aerosol water content is generally below $10^{-12} \text{ m}^3(\text{aq})/\text{m}^3(\text{air})$.

3 Results and Discussion

3.1 Aerosol distribution

The distribution of sea salt aerosol strongly influences the release of bromine to the gas phase. Therefore its representation by M7 and the source and sink processes in MESSy are analysed in the following.

Figure 1 displays the annually averaged global sources and sinks. The panel on the upper left shows the sea salt emissions in $\text{g}/(\text{m}^2\text{yr})$. The largest emissions occur in the

mid-latitudes over the ocean, i.e. in the storm track regions. The high prevailing wind speeds lead to strong sea salt production. The smallest emissions over the ocean are found in the tropics west of the continents and throughout Polynesia.

Due to the short atmospheric lifetime of coarse mode sea salt particles, the spatial distribution of the sinks is highly correlated to the source distribution. The largest spatial gradients appear in the dry deposition process (upper right), showing the highest loss rate in the mid-latitudes and the lowest in the tropics. The storm track regions are associated with high wind speeds, hence the strongest dry deposition appears in these regions. The largest wet deposition events (lower right) occur also in the storm track regions, as wet deposition is strongest in regions where precipitation events are frequent. Although sedimentation (lower left) follows the same pattern as the other three processes, the gradient from the mid-latitudes to the tropics is relatively small. Since sedimentation only depends on the physical properties of the particles and on the density of the ambient air the efficiency of sedimentation is not as strongly related to wind speed as dry deposition.

Table 3 lists the annually integrated global source and sink fluxes for all M7 components in Tg/yr. The sulphate emissions are zero, because primary emissions are not taken into account. The largest and the smallest sink are wet deposition and sedimentation, respectively, except for dust for which the smallest sink is dry deposition. This is on the one hand in contrast to [Pierce and Adams \(2006\)](#) reporting dry deposition fluxes (including sedimentation) to be larger than wet deposition fluxes. On the other hand, [Textor et al. \(2006\)](#) state that “Models do neither agree on the split between wet and dry deposition, nor on that between sedimentation and other dry deposition processes.”, thus our results are not more or less realistic than other aerosol dynamical models. A detailed analysis of the complete aerosol distribution simulated by this M7 implementation will be given in a follow-up paper. Here we only analyse the sea salt distribution which is important for the bromine release to the gas phase.

The simulated burden (7.3 Tg) and the lifetime (0.6 days) of sea salt seem to be relatively low but they match the AeroCom median (7.5 Tg/ 0.5 days) very well ([Textor et al.](#),

**Part-I: model
description, sea salt
aerosols and pH**A. Kerkweg et al.

Title Page

Abstract

Introduction

Conclusions

References

Tables

Figures

◀

▶

◀

▶

Back

Close

Full Screen / Esc

Printer-friendly Version

Interactive Discussion



2006). Depending on the emission function [Pierce and Adams \(2006\)](#) report sea salt burdens (lifetimes) ranging from 1.8 to 17.0 Tg (0.46 to 2.72 days). In view of the burden our model is well within this range, but the lifetime is near the lower end. An often used assumption for the lifetime of coarse mode sea salt is 2 days ([Sander and Crutzen, 1996](#)). [Stier et al. \(2005\)](#) report a burden/lifetime of 10.5 Tg/0.8 days. The differences between the burdens/lifetimes of [Stier et al. \(2005\)](#) and our simulation are also apparent when comparing the annually averaged vertically integrated column mass (their Fig. 2 to our Fig. 2). ECHAM5-HAM reaches values between 20 and 50 mg/m² in most oceanic regions, exceeded by some regions where concentration between 50 and 100 mg/m² occur. E5/M1⁺ ranges between 10 and 50 mg/m² over the ocean. However, the patterns of the distribution are very similar. Since ECHAM5-HAM and E5/M1⁺ use the same microphysical core of the aerosol model and the same sea salt emission function these differences are caused by more efficient sink processes in E5/M1⁺. Here, especially the treatment of the wet deposition as the dominant sink is important. Since the MESSy implementation describes the process in more detail differences in the efficiency of this process were expected. In our case the implementation of MESSy leads to a higher loss rate which might be true or overestimated. Since the sea salt lifetime has only been crudely estimated so far, the shorter sea salt lifetimes in our simulation and in the AeroCom median may be closer to reality than the earlier estimate cited above. The lifetime influences the aerosol pH especially in regions with low gas phase acid concentrations. Hence the time available for acidification of the aerosol is significantly smaller in models using the assumption of a sea salt lifetime of 2 days.

It is rather difficult to compare simulation results to measurements and this is even harder for a relatively coarse model resolution. Measurements are mostly taken at single, distinct locations, whereas the model grid box represents approximately 250 km×250 km and averages over this area. Nevertheless, some comparisons are presented in the following. Most data are obtained in measurement campaigns limited to a specific region and to a time frame of a few weeks. Additionally, many measurements have a cutoff diameter of 10 μm. Thus the measured mass is likely smaller than

**Part-I: model
description, sea salt
aerosols and pH**A. Kerkweg et al.

[Title Page](#)[Abstract](#)[Introduction](#)[Conclusions](#)[References](#)[Tables](#)[Figures](#)[⏪](#)[⏩](#)[◀](#)[▶](#)[Back](#)[Close](#)[Full Screen / Esc](#)[Printer-friendly Version](#)[Interactive Discussion](#)

**Part-I: model
description, sea salt
aerosols and pH**A. Kerkweg et al.

Title Page

Abstract

Introduction

Conclusions

References

Tables

Figures

◀

▶

◀

▶

Back

Close

Full Screen / Esc

Printer-friendly Version

Interactive Discussion



in reality and the largest particles are expected to relatively strongly influence the mean mass concentration. Lewis and Schwartz (2004) review measurements and model results related to sea salt. Their Fig. 17 displays measurements of sea salt aerosol mass concentrations as a function of the 10 m wind speed. Most of the measurements are in the range of 5 to 100 $\mu\text{g}/\text{m}^3$, and the simulated sea salt mass concentrations of this study shown in Fig. 3, seem to correspond well to the extent that the data sets are comparable. Phinney et al. (2006) report a mean mass concentration of 2.4 $\mu\text{g}/\text{m}^3$ for the north east Pacific Ocean. This is substantially lower than in our model which predicts values between 5 and 20 $\mu\text{g}/\text{m}^3$. Fitzgerald (1991) reports in his review typical concentrations between 2 and 50 $\mu\text{g}/\text{m}^3$ for coarse mode aerosol over the remote ocean, which in turn matches our simulation.

Many aerosol measurements are made available by AeroCom (<http://nansen.ipsl.jussieu.fr/AEROCOM/>). Here we focus on three projects in which sea salt aerosol concentrations have been measured: the IMPROVE network (http://vista.cira.colostate.edu/improve/Data/IMPROVE/improve_data.htm), the EMEP network (http://www.emep.int/index_data.html), and the AEROCE network (<http://www.igac.noaa.gov/newsletter/24/aeroce.php>).

At the continental locations in North America (IMPROVE network, not shown here) our sea salt concentrations are consistently much higher than those observed. We expect this to be related to the coarse model resolution, because spatial averaging over 250km \times 250km grid cells unrealistically assumes the transport of coarse mode particles up to 250km from the coast within one model timestep.

Figure 4 shows the comparison for all EMEP stations providing sea salt mass measurements. For the near sea level stations the simulations matches the observations well, but for all stations located in higher altitudes the simulation overestimates the amount of available sea salt mass.

The picture is not quite as clear for the comparison with the AEROCE data, mostly comprising stations located at the coast or on islands. Figure 5 depicts the AEROCE stations ordered from north to south. In contrast to the EMEP data comparison the sea

salt concentration is underestimated for the two northernmost stations Heimaey and Mace Head. For the stations located around 30°N the simulation reproduces the sea salt abundance as well as the annual cycle. At low latitudes no systematic deviations are apparent. For the western Pacific stations, Enewetak Atoll and Nauru, the simulation strongly underestimates the sea salt abundance, whereas for the stations in the eastern Pacific, Fanning Island and Tutuila, it overestimates it. Both effects might be attributed to local effects which are not included in the global model. In the southern hemispheric mid-latitudes the simulation mostly overestimates the sea salt abundance. For Antarctica (Palmer Station) the annual variability is overestimated, but the annual cycle is clear in the observations as well as in the simulation. To summarise, the model seems to overestimate the sea salt concentrations over the continents. This is partly related to the coarse resolution of the model.

Number concentrations of coarse mode aerosol are reported more often than sea salt masses. Large particles form by primary emissions of sea salt and dust, and by growth of smaller particles, e.g., by sulphate condensation, by coagulation or by evaporation of droplets. Consequently, in the representation of the submodel M7 these particles consist not only of sea salt and dust, but also of organic matter, black carbon and sulphate. The growth of smaller particles into the accumulation mode mainly determines the particle number in this size range, yielding relatively high numbers. However, the number concentration of coarse mode particles is mainly driven by primary emissions. Additionally processing of aerosols by clouds leads to formation of large aerosol particles. Figure 6 shows the simulated annually averaged number concentration of the coarse mode aerosol. In case of cloud evaporation all resulting aerosol particles are put into the coarse mode as sulphate emissions are high over Europe, the large maximum in this region is most probably an artefact of this parameterisation.

Lewis and Schwartz (2004) report number concentrations ranging from below 1 cm⁻³ up to a maximum of 200 cm⁻³. This is in good correspondence with the simulated concentrations. Most of the oceanic measurements reviewed by Lewis and Schwartz (2004) are between 1 cm⁻³ and 20 cm⁻³, which agrees also well with the annual mean

**Part-I: model
description, sea salt
aerosols and pH**A. Kerkweg et al.

[Title Page](#)[Abstract](#)[Introduction](#)[Conclusions](#)[References](#)[Tables](#)[Figures](#)[⏪](#)[⏩](#)[◀](#)[▶](#)[Back](#)[Close](#)[Full Screen / Esc](#)[Printer-friendly Version](#)[Interactive Discussion](#)

number concentrations in our simulation.

An additional difficulty in comparing field data with model results is that most of the time the measured and the simulated radii intervals do not exactly match. Furthermore, the measurements are associated with some uncertainties. For example, a time dependence seems to be evident with smaller number concentrations reported in the literature in the early studies increasing to larger ones in more recent studies. Small numbers were reported in the 1970s and 1980s from $<1 \text{ cm}^{-3}$ up to 10 cm^{-3} as an upper limit (for details see [Lewis and Schwartz, 2004](#)). More recent studies presented higher concentrations. [O'Dowd and Smith \(1993\)](#) measured concentrations in the range of 2 cm^{-3} to 80 cm^{-3} in October/November 1989 over the north-east Atlantic for sea salt aerosols ranging from $0.01 \mu\text{m}$ to $3 \mu\text{m}$. Hence, the measured number concentrations correspond to the sum of the number concentrations of the coarse and the accumulation mode. Figure 7 shows the sum of the seasonally averaged number concentrations of the accumulation and the coarse mode. These number concentrations closely correspond to the observations. From the figures shown by [O'Dowd and Smith \(1993\)](#), a mean particle number concentration for coarse mode aerosol ($0.6 \mu\text{m}$ – $3 \mu\text{m}$) of around 5 cm^{-3} – 10 cm^{-3} can be deduced. For the northeastern Atlantic our model predicts concentrations between 1 cm^{-3} and 5 cm^{-3} , thus slightly lower than the observations. [O'Dowd \(2002\)](#) reports a rather constant concentration of 50 cm^{-3} of particles larger than $0.3 \mu\text{m}$ at the Irish coast. This relatively high concentrations should be mostly attributed to a coastal effect (e.g. enhanced wave breaking), which can currently not be resolved in a global model. [Bates et al. \(1998\)](#) and [Murphy et al. \(1998\)](#) both published measurements from ACE 1 (the First Aerosol Characterisation Experiment). ACE 1 took place from 15 November to 14 December 1995, in a region south-south-east of Tasmania, Australia in the Southern Ocean. Even though taking part in the same campaign they report different results. [Bates et al. \(1998\)](#) measured number concentrations of about 15 cm^{-3} in clean marine air and 23 cm^{-3} in continentally influenced air for particles larger than $0.3 \mu\text{m}$. [Murphy et al. \(1998\)](#) report concentrations of 30 cm^{-3} for particles larger than $0.16 \mu\text{m}$. Both particle ranges include

**Part-I: model
description, sea salt
aerosols and pH**

A. Kerkweg et al.

Title Page

Abstract

Introduction

Conclusions

References

Tables

Figures

◀

▶

◀

▶

Back

Close

Full Screen / Esc

Printer-friendly Version

Interactive Discussion



parts of the M7 accumulation mode. Thus, since Fig. 6 shows smaller concentrations for coarse mode aerosol only and Fig. 7 larger values for the sum of accumulation and coarse mode particles, our simulation results fit within the range of the measurements. Guazzotti et al. (2001) measured aerosols during the Indian Ocean Experiment from February to March 1999 and observed a range from less than 1 cm^{-3} to 5 cm^{-3} . The model simulates concentrations between 1 cm^{-3} to 10 cm^{-3} , i.e., slightly higher than the measurements.

To summarise, the model is in reasonable agreement with the reported measurements taking into account the model's limitations and the uncertainties of observations. The model tends to slightly overestimate the mass and to slightly underestimate the number concentrations of sea salt aerosol.

3.2 Coarse Mode Aerosol pH

The aerosol pH is a key driver of aerosol chemistry. Keene et al. (1998) point out its importance for sulphate oxidation and for dehalogenation: at pH 8 the reaction of sulphur(IV) with ozone is dominant, at pH 5.5 oxidation by HOCl and H_2O_2 prevails and at pH 3 the decreased effective SO_2 solubility slows down the oxidation to sulphur(VI). The amount of HCl release changes drastically between pH 5.5 and 3, whereas the release of bromine is relatively constant and very efficient in this pH range. For aerosols containing chlorine the HCl/ Cl^- buffer is important for the aerosol pH (Fridlind and Jacobson, 2000; Keene and Savoie, 1998).

The aerosol pH is rather difficult to measure. Only a few direct measurements of diluted aerosol samples exist (Keene et al., 2002, 2004). In most cases the aerosol pH – if reported at all – is estimated by assuming the aerosol to be in thermodynamical equilibrium (Keene et al., 1998; Fridlind and Jacobson, 2000). Based on this assumption an aerosol pH for each acid measured in gas and aqueous phase can be calculated. The disadvantage of this method is that the calculated pH depends on the respective acid (Keene et al., 2004). Another approach is to include all measured concentrations in an equilibrium (box-)model for the calculation of a single mean pH value. Fridlind

Part-I: model description, sea salt aerosols and pH

A. Kerkweg et al.

Title Page

Abstract

Introduction

Conclusions

References

Tables

Figures

◀

▶

◀

▶

Back

Close

Full Screen / Esc

Printer-friendly Version

Interactive Discussion



and Jacobson (2000) used the thermodynamical equilibrium model EQUISOLVII for this purpose. But the assumption of thermodynamical equilibrium is a simplification, Keene et al. (2004) state that phase disequilibria cause negative deviations in median pH values. But these phase disequilibria only occur for sea salt aerosol particle diameters larger than 2.8 μm . Unfortunately, because of these difficulties in measuring aerosol pH, only few measurements are available. They are shown in Table 4.

Figure 8 shows the simulated annual average of the aerosol pH in the marine boundary layer. Due to numerical reasons the aerosol chemistry was only calculated when the liquid water content was above $10^{-12} \text{ m}^3/\text{m}^3$. Consequently, the pH calculation is -in fact- restricted to the marine boundary layer. In general the pH is lower in the northern hemisphere. This is a direct consequence of the higher abundance of acids in the northern hemisphere where the largest emissions of acid precursors take place, e.g. in large urban areas, by power-plants and industries. The highest pH values are reached in the southern ocean storm track – the dominant source region for sea salt aerosol. Freshly emitted sea salt aerosol is alkaline and the abundance of gas phase acids is relatively low in the southern hemisphere; thus the southern storm tracks stand out because of high aerosol pH. The source of alkalinity is not much smaller in the northern storm tracks, but there titration by acids reduces the pH. Not surprisingly, the outflow regions of the continents show the lowest pH values.

The seasonal differences of the aerosol pH are shown in Fig. 9. The aerosol in each hemisphere is more strongly acidified by approximately 2 pH units in the respective spring/summer than in the winter season. In spring/summer surface winds are weaker leading to less efficient exchange processes (sources as well as sinks) and consequently to a longer residence time for the aerosol resulting in higher acidification. In the southern hemispheric winter strong emissions in the southern ocean storm tracks and the lower abundance of gas phase acids lead to slightly alkaline ($\text{pH}\approx 8$) aerosol. In contrast, the aerosol is slightly acidified ($\text{pH}\approx 6$) in the same region in summer. In the northern hemisphere the aerosol is acidified throughout the year reaching pH values as low as 4 in spring and up to 6 in winter.

Part-I: model description, sea salt aerosols and pHA. Kerkweg et al.

Title Page

Abstract

Introduction

Conclusions

References

Tables

Figures

◀

▶

◀

▶

Back

Close

Full Screen / Esc

Printer-friendly Version

Interactive Discussion



**Part-I: model
description, sea salt
aerosols and pH**

A. Kerkweg et al.

[Title Page](#)[Abstract](#)[Introduction](#)[Conclusions](#)[References](#)[Tables](#)[Figures](#)[⏪](#)[⏩](#)[◀](#)[▶](#)[Back](#)[Close](#)[Full Screen / Esc](#)[Printer-friendly Version](#)[Interactive Discussion](#)

Averages of pH values, however, do not provide the full picture. Therefore, we additionally show frequency distributions of pH values. The bars are scaled with the number of events and normalised to 100%. Figures 10 and 11 show frequency distributions of the pH at two distinct locations for four selected months to visualise the seasonal cycle of sea salt aerosol pH and the frequency of occurrence of particular pH values. The first gridbox (170°W, 55°N) is located in the middle of the North Atlantic ocean. This region is influenced by the outflow of North America. This leads to relatively low pH values and little variation in the pH distribution throughout the year. The lowest pH values occur in March, where the sea salt pH is 4 or less most of the time. The highest pH values occur in December. At this time of the year the wind speed and sea salt emissions are strongest leading to a stronger alkalinity source.

The second series of frequency distributions (Fig. 11) refers to the southern ocean storm track region (100°E, 50°S). In the southern hemispheric winter (June to October) the aerosol is neutral (almost alkaline). The aerosol is slightly acidified throughout the rest of the year with lowest values (of around 5) in the southern hemispheric autumn.

Figure 12 shows a frequency distribution of pH values along a north-south transect at 170°W over the Atlantic ocean from 55°N to the Equator. A distinct gradient from north to south is apparent in the spectrum of pH values. The pH variability is much higher in the North covering a pH range of 1 to 7. In contrast, south of 25°N the pH values only vary between pH 4 and 6. Even if the variability is high, the average pH values do not differ much: all averages range between 4.5 and 4.8.

Figure 13 shows frequency distributions for the region and time of the year of the measurement campaigns as listed in the attached table. Since we did not simulate the same years, we show model results for the year 2000.

Keene and Savoie (1999) report measurements of pH 3.5 to 4.5 for a site located directly at the coast of Bermuda, obtained in a campaign during April and May 1996. The simulated average pH of 3.5 is at the lower end of this measured range, but the distribution is narrow, in accordance to the narrow pH interval reported by Keene and Savoie (1999).

During a campaign in May 1997 at the same site aerosol pH values ranged from approximately 3.5 to 5.3 (Keene et al., 2002). The simulation again yields pH values near the lower end of the measurements. The simulated width of the distribution is equally small as for the first campaign.

5 Fridlind and Jacobson (2000) estimated coarse mode aerosol pH ranging from 2 to 5 from the measurements made during ACE 1. Our simulation reproduces the wider range of acidification, but with an average pH of 6 the simulated aerosol pH is beyond the maximum value of the measurements.

10 Pszenny et al. (2004) report measurements at Hawaii, USA, in September 1999 with pH values ranging from 4.5 to 5.4. The simulation underestimates the pH values slightly, though reproduce the small standard deviation and a narrow modal distribution.

At the US east coast Keene et al. (2004) measured an aerosol pH of around 1.9–3.3 for the aerosol size ranges which correspond to the coarse mode in the model. In this case the simulation reproduces very well the reported measurements.

15 The simulated pH values are slightly lower compared to Keene and Savoie (1999); Keene et al. (2002) and Pszenny et al. (2004), whereas they are close to the maximum reported by Keene et al. (2004) and higher than the maximum compared to Fridlind and Jacobson (2000). Since the first four publications use basically the same method to determine the aerosol pH and Fridlind and Jacobson (2000) use an equilibrium model, the differences might be explained by the uncertainties in the analysis of “measured” pH. On the other hand, simulation results are shown for the year 2000 instead of the years of the respective campaigns. Given all these uncertainties in the simulation as well as in the measurements, we consider the sea salt aerosol pH to be reasonably well reproduced in our simulation.

25

Part-I: model description, sea salt aerosols and pH

A. Kerkweg et al.

Title Page

Abstract

Introduction

Conclusions

References

Tables

Figures

◀

▶

◀

▶

Back

Close

Full Screen / Esc

Printer-friendly Version

Interactive Discussion



4 Conclusions

We present first results of a comprehensive AC-GCM simulation including gas and aerosol phase chemistry. Since this simulation aims at representing bromine chemistry and the largest boundary layer source of bromine is release from aerosol particles, we focus on the aerosol mass, number distributions and the aerosol pH in this first part of a series of articles. In our analysis we focus on coarse mode aerosols, because we had to limit the explicit chemistry calculation to one mode for numerical reasons. Since the coarse mode is the most important one for sea salt, it is reasonable to neglect the fine modes in this first global study.

Sea salt mass concentrations are overall slightly higher in the simulation compared to the observations. This can largely be attributed to the coarse model resolution. An additional, but minor effect is that many instruments have a cutoff diameter of 10 (or 25) μm resulting in an underestimation of sea salt mass abundance. In contrast to this, the number concentrations are mostly underestimated by the model. The mean lifetime of coarse mode sea salt of 0.5 days derived from our simulation agrees very well with the AeroCom median.

It is difficult to measure the sea salt pH, and only a few observations are available. Furthermore, pH measurements are associated with large uncertainties and based on assumptions, such as thermodynamical equilibrium of the particle and for the effective Henry's law coefficient. Especially for the relatively large sea salt particles, the equilibrium assumption may be violated on time scales smaller than 1 h. We conclude that within the range of these uncertainties the simulated aerosol pH values sufficiently accurately reproduce the observations.

In summary, the basis for the simulation of aerosol phase chemistry and thus for bromine release from sea salt aerosol is provided by our model. In the following publications within this series the bromine chemistry of the marine aerosol will be analysed in detail.

Acknowledgements. We thank all MESSy developers for cooperation and support. The authors

Part-I: model description, sea salt aerosols and pH

A. Kerkweg et al.

Title Page

Abstract

Introduction

Conclusions

References

Tables

Figures

◀

▶

◀

▶

Back

Close

Full Screen / Esc

Printer-friendly Version

Interactive Discussion



thank the “application support for high computer performance” team of the MPG computer center Garching, in particular I. Weidl, R. Hatzky, W. Nagel and H. Lederer. We are grateful for the availability of the observational data through the AeroCom data compilation by S. Guibert (LSCE/IPSL, France) and in particular all scientists and technicians contributing to the data collection within EMEP, IMPROVE and AEROCE. We have used the Ferret program (<http://www.ferret.noaa.gov>) from NOAA’s Pacific Marine Environmental Laboratory for creating the graphics in this paper.

References

- Balkanski, Y., Schulz, M., Claquin, T., Moulin, C., and Ginoux, P.: Global emissions of mineral aerosol: Formulation and validation using satellite imagery, chap. Emission of Atmospheric Tracer Compounds, pp. 253–282, Kluwer Acad., Norwell, Mass., 2003. [7226](#)
- Bates, T. S., Kapustin, V. N., Quinn, P. K., Covert, D. S., Coffman, D. J., Mari, C., Dirkee, P. A., Bruyn, W. J. D., and Saltzman, E. S.: Processes controlling the distribution of aerosol particles in the lower marine boundary layer during the First Aerosol Characterization Experiment (ACE1), *J. Geophys. Res.*, 103, 16 369–16 383, 1998. [7233](#)
- Brasseur, G. P. and Solomon, S.: *Aeronomy of the middle atmosphere*, Springer-Verlag, Dordrecht, The Netherlands, 2005. [7218](#)
- Damian, V., Sandu, A., Damian, M., Potra, F., and Carmichael, G. R.: The kinetic preprocessor KPP – a software environment for solving chemical kinetics, *Comp. Chem. Eng.*, 26, 1567–1579, 2002. [7227](#)
- Dentener, F., Kinne, S., Bond, T., Boucher, O., Cofala, J., Generoso, S., Ginoux, P., Gong, S., Hoelzemann, J. J., Ito, A., Marelli, L., Penner, J. E., Putaud, J.-P., Textor, C., Schulz, M., van der Werf, G. R., and Wilson, J.: Emissions of primary aerosol and precursor gases in the years 2000 and 1750 prescribed data-sets for AeroCom, *Atmos. Chem. Phys.*, 6, 4321–4344, 2006, <http://www.atmos-chem-phys.net/6/4321/2006/>. [7225](#)
- Fitzgerald, J. W.: *Marine Aerosols: A Review*, *Atmos. Environ.*, 25A, 533–545, 1991. [7231](#)
- Fridlind, A. and Jacobson, M.: A study of gas-aerosol equilibrium and aerosol pH in the remote marine boundary layer during the First Aerosol Characterization Experiment (ACE 1), *J. Geophys. Res.*, 105, 17 325–17 340, 2000. [7234](#), [7237](#), [7248](#)

Part-I: model description, sea salt aerosols and pH

A. Kerkweg et al.

Title Page

Abstract

Introduction

Conclusions

References

Tables

Figures

◀

▶

◀

▶

Back

Close

Full Screen / Esc

Printer-friendly Version

Interactive Discussion



**Part-I: model
description, sea salt
aerosols and pH**

A. Kerkweg et al.

Title Page

Abstract

Introduction

Conclusions

References

Tables

Figures

◀

▶

◀

▶

Back

Close

Full Screen / Esc

Printer-friendly Version

Interactive Discussion

Ganzeveld, L. and Lelieveld, J.: Dry deposition parameterization in a chemistry general circulation model and its influence on the distribution of reactive trace gases, *J. Geophys. Res.*, 100, 20 999–21 012, 1995. [7226](#)

Giorgetta, M. A., Manzini, E., and Roeckner, E.: Forcing of the quasi-biennial oscillation from a broad spectrum of atmospheric waves, *Geophys. Res. Lett.*, 29, doi:10.1029/2002GL014756, 2002. [7221](#)

Giorgetta, M. A., Manzini, E., Roeckner, E., m. Esch, and Bengtson, L.: Climatology and forcing of the quasi-biennial oscillation in the MAECHAM5 model, *J. Clim.*, 19, 3882–3901, 2006. [7221](#)

Gong, S. L., Barrie, L. A., Blanchet, J.-P., von Salzen, K., Lohmann, U., Lesins, G., Spacek, L., Zhang, L. M., Girard, E., Lin, H., Leaitch, R., Leighton, H., Chylek, P., and Huang, P.: Canadian Aerosol Module: A size-segregated simulation of atmospheric aerosol processes for climate and air quality models 1. Module development, *J. Geophys. Res.*, 108, doi:10.1029/2001JD002002, 2003. [7219](#)

Guazzotti, S. A., Coffee, K. R., and Parther, K. A.: Continuous measurements of size-resolved particle chemistry during INDOEX-Intensive Field Phase 99, *J. Geophys. Res.*, 106, 28 607–28 627, 2001. [7234](#)

Guelle, W., Schulz, M., Balkanski, Y., and Dentener, F.: Influence of the source formulation on modeling the atmospheric global distribution of sea salt aerosol, *J. Geophys. Res.*, 106, 27 509–27 524, 2001. [7225](#)

Jeuken, A., Siegmund, P., Heijboer, L., Feichter, J., and Bengtson, L.: On the potential of assimilating meteorological analysis in a climate model for the purpose of model validation, *J. Geophys. Res.*, 101, 16 939–16 950, 1996. [7221](#)

Jöckel, P., Sander, R., Kerkweg, A., Tost, H., and Lelieveld, J.: Technical Note: The Modular Earth Submodel System (MESSy) - a new approach towards Earth System Modeling, *Atmos. Chem. Phys.*, 5, 433–444, 2005, <http://www.atmos-chem-phys.net/5/433/2005/>. [7220](#)

Jöckel, P., Tost, H., Pozzer, A., Brühl, C., Buchholz, J., Ganzeveld, L., Hoor, P., Kerkweg, A., Lawrence, M. G., Sander, R., Steil, B., Stiller, G., Tanarhte, M., Taraborrelli, D., van Aardenne, J., and Lelieveld, J.: The atmospheric chemistry general circulation model ECHAM5/MESSy1: Consistent simulation of ozone from the surface to the mesosphere, *Atmos. Chem. Phys.*, 6, 5067–5104, 2006, <http://www.atmos-chem-phys.net/6/5067/2006/>. [7219](#), [7220](#), [7221](#), [7222](#), [7223](#)



**Part-I: model
description, sea salt
aerosols and pH**

A. Kerkweg et al.

Title Page

Abstract

Introduction

Conclusions

References

Tables

Figures

◀

▶

◀

▶

Back

Close

Full Screen / Esc

Printer-friendly Version

Interactive Discussion

- Keene, W. and Savoie, D.: The pH of deliquesced sea-salt aerosol in polluted air, *Geophys. Res. Lett.*, 25, 2181–2184, 1998. [7234](#)
- Keene, W. and Savoie, D.: Correction to "The pH of deliquesced sea-salt aerosol in polluted air", *Geophys. Res. Lett.*, 26, 1315–1316, 1999. [7236](#), [7237](#), [7248](#)
- 5 Keene, W., Pszenny, A., Maben, J., Stevenson, E., and Wall, A.: Closure evaluation of size-resolved aerosol pH in the New England coastal atmosphere during summer, *J. Geophys. Res.*, 109, doi:10.1029/2004JD004801, 2004. [7234](#), [7235](#), [7237](#), [7248](#)
- Keene, W. C., Sander, R., Pszenny, A. A., Vogt, R., Crutzen, P. J., and Galloway, J. N.: Aerosol pH in the marine boundary layer: A review and model evaluation, *J. Aerosol Sci.*, 29, 339–
10 356, 1998. [7234](#)
- Keene, W. C., Pszenny, A. A. P., Maben, J. R., and Sander, R.: Variation of marine aerosol acidity with particle size, *Geophys. Res. Lett.*, 29, doi:10.1029/2001GL013881, 2002. [7234](#),
[7237](#), [7248](#)
- Kerkweg, A., Buchholz, J., Ganzeveld, L., Pozzer, A., Tost, H., and Jöckel, P.: Technical Note: an implementation of the dry removal processes DRY DEPosition and SEDimentation in the Modular Earth Submodel System (MESSy), *Atmos. Chem. Phys.*, 6, 4617–4632, sRef-ID: 1680-7324/acp/2006-6-4617, 2006a. [7222](#), [7226](#)
- Kerkweg, A., Sander, R., Tost, H., and Jöckel, P.: Technical Note: Implementation of prescribed (OFFLEM), calculated (ONLEM), and pseudo-emissions (TNUDGE) of chemical species in the Modular Earth Submodel System (MESSy), *Atmos. Chem. Phys.*, 6, 3603–3609, 2006b.
20 [7222](#), [7226](#)
- Kerkweg, A., Sander, R., Tost, H., Jöckel, P., and Lelieveld, J.: Technical Note: simulation of detailed aerosol chemistry on the global scale using MECCA-AERO, *Atmos. Chem. Phys.*, 7, 2973–2985, 2007,
25 <http://www.atmos-chem-phys.net/7/2973/2007/>. [7219](#), [7222](#), [7224](#), [7227](#), [7228](#)
- Landgraf, J. and Crutzen, P.: An Efficient Method for Online Calculation of Photolysis and Heating Rates, *J. Atmos. Sci.*, 55, 863–878, 1998. [7222](#)
- Lauer, A., Hendricks, J., Ackermann, I., Schell, B., Hass, H., and Metzger, S.: Simulating aerosol microphysics with ECHAM/MADE GCM- Part I: Model description and comparison with observations, *Atmos. Chem. Phys.*, 5, 3251–3276, 2005,
30 <http://www.atmos-chem-phys.net/5/3251/2005/>. [7219](#)
- Lewis, E. R. and Schwartz, S. E.: Sea Salt Aerosol Production: Mechanisms, Methods, Measurements and Models - A Critical Review, American Geophysical Union. Washington, DC,



2004. [7231](#), [7232](#), [7233](#)

Monahan, E. C.: The Role of Air-Sea Exchange in Geochemical Cycling, chap. The Ocean as a Source for Atmospheric Particles, pp. 129–163, D. Reidel Publishing Company, 1986. [7225](#)

Murphy, D., Thomson, D., Middlebrook, A., and Schein, M.: In situ single-particle characterization at Cape Grim, *J. Geophys. Res.*, 103, 16 485–16 491, 1998. [7233](#)

O’Dowd, C. D.: On the spatial extent and evolution of coastal aerosol plumes, *J. Geophys. Res.*, 107, 8105, doi:10.1029/2001JD000422, 2002. [7233](#)

O’Dowd, C. D. and Smith, M. H.: Physicochemical Properties of Aerosols Over the Northeast Atlantic: Evidence for Wind-Speed-Related Submicron Sea-Salt Aerosol Production, *J. Geophys. Res.*, 98, 1137–1149, 1993. [7233](#)

Phinney, L., Leaitch, W. R., Lohmann, U., Boudires, H., Worsnop, D. R., Jayne, J. T., Toom-Saunty, D., Wadleigh, M., Sharma, S., and Shantz, N.: Characterization of the aerosol over the sub-arctic north east Pacific Ocean, *Deep-Sea Res.*, 53, 2410–2433, 2006. [7231](#)

Pierce, J. R. and Adams, P. J.: Global evaluation of CCN formation by direct emission of sea salt and growth of ultrafine sea salt, *J. Geophys. Res.*, doi:10.1029/2005JD006186, 2006. [7229](#), [7230](#)

Pozzer, A., Jöckel, P., Sander, R., William, J., Ganzeveld, L., and Lelieveld, J.: Technical Note: The MESSy-submodel AIRSEA calculating the air-sea exchange of chemical species, *Atmos. Chem. Phys.*, 6, 5435–5444, 2006, <http://www.atmos-chem-phys.net/6/5435/2006/>. [7222](#)

Pozzer, A., Jöckel, P., Tost, H., Sander, R., Ganzeveld, L., Kerkweg, A., and Lelieveld, J.: Simulating organic species with the global atmospheric chemistry general circulation model ECHAM5/MESSy1: a comparison of model results with observations, *Atmos. Chem. Phys.*, 7, 2527–2550, 2007, <http://www.atmos-chem-phys.net/7/2527/2007/>. [7222](#)

Pruppacher, H. and Klett, J.: *Microphysics of Clouds and Precipitation*, 2nd edition, Kluwer, Dordrecht, 954 pp., 1997. [7226](#)

Pszenny, A. A. P., Moldanová, J., Keene, W. C., Sander, R., Maben, J. R., Martinez, M., Crutzen, P. J., Perner, D., and Prinn, R. G.: Halogen cycling and aerosol pH in the Hawaiian marine boundary layer, *Atmos. Chem. Phys.*, 4, 147–168, 2004, <http://www.atmos-chem-phys.net/4/147/2004/>. [7237](#), [7248](#)

Roeckner, E., Bäuml, G., Bonaventura, L., Brokopf, R., Esch, M., Giorgetta, M., Hagemann, S., Kirchner, I., Kornblueh, L., Manzini, E., Rhodin, A., Schlese, U., Schulzweida, U., and

**Part-I: model
description, sea salt
aerosols and pH**

A. Kerkweg et al.

Title Page

Abstract

Introduction

Conclusions

References

Tables

Figures

◀

▶

◀

▶

Back

Close

Full Screen / Esc

Printer-friendly Version

Interactive Discussion



**Part-I: model
description, sea salt
aerosols and pH**

A. Kerkweg et al.

Title Page

Abstract

Introduction

Conclusions

References

Tables

Figures

◀

▶

◀

▶

Back

Close

Full Screen / Esc

Printer-friendly Version

Interactive Discussion



Tompkins, A.: The atmospheric general circulation model ECHAM5, Tech. rep., Max Planck-Institute for Meteorology, 2003. [7220](#)

Roeckner, E., Brokopf, R., Esch, M., Giorgetta, M., Hagemann, S., Kornblueh, L., Manzini, E., Schlese, U., and Schulzweida, U.: The atmospheric general circulation model ECHAM5. PART II: Sensitivity of Simulated Climate to Horizontal and Vertical Resolution, Tech. Rep. MPI-Report 354, Max Planck-Institute for Meteorology, http://www.mpimet.mpg.de/fileadmin/publikationen/Reports/max_scirep_354.pdf, 2004. [7220](#)

Sander, R. and Crutzen, P.: Model study indicating halogen activation and ozone destruction in polluted air masses transported to the sea, *J. Geophys. Res.*, 101, 9121–9138, 1996. [7230](#)

Sander, R., Keene, W., Pszenny, A., Arimoto, R., Ayers, G., Baboukas, E., Cainey, J., Crutzen, P., Duce, R., Hönninger, G., Huebert, B., Maenhaut, W., Mihalopoulos, N., Turekian, V., and Dingenen, R. V.: Inorganic bromine in the marine boundary layer: a critical review, *Atmos. Chem. Phys.*, 3, 1301–1336, 2003, <http://www.atmos-chem-phys.net/3/1301/2003/>. [7218](#)

Sander, R., Kerkweg, A., Jöckel, P., and Lelieveld, J.: Technical Note: The new comprehensive atmospheric chemistry module MECCA, *Atmos. Chem. Phys.*, 5, 445–450, 2005, <http://www.atmos-chem-phys.net/5/445/2005/>. [7222](#)

Sandu, A. and Sander, R.: Technical note: Simulating chemical systems in Fortran90 and Matlab with the Kinetic PreProcessor KPP-2.1, *Atmos. Chem. Phys.*, 6, 187–195, 2006, <http://www.atmos-chem-phys.net/6/187/2006/>. [7227](#)

Schulz, M., de Leeuw, G., and Balkanski, Y.: Emission of atmospheric trace compounds, chap. Sea-salt aerosol source functions and emissions, pp. 333–359, Ed. Kluwer, 2004. [7225](#)

Slinn, S. and Slinn, W.: Predictions for Particle Deposition on Natural Waters, *Atmos. Environ.*, 14, 1013–1016, 1980. [7226](#)

Smith, M. H. and Harrison, M.: The Sea Spray Generation Function, *J. Aerosol Sci.*, 29, S189–S190, suppl.1, 1998. [7225](#)

Spracklen, D. V., Pringle, K. J., Carslaw, K. S., Chipperfield, M. P., and Mann, G. W.: A global off-line model of size-resolved aerosol microphysics: I. Model development and prediction of aerosol properties, *Atmos. Chem. Phys.*, 5, 2227–2252, 2005, <http://www.atmos-chem-phys.net/5/2227/2005/>. [7219](#)

Stier, P., Feichter, J., Kinne, S., Kloster, S., Vignati, E., Wilson, J., Ganzeveld, L., Tegen, I., Werner, M., Balkanski, Y., Schulz, M., and Boucher, O.: The Aerosol-Climate Model ECHAM5-HAM, *Atmos. Chem. Phys.*, 5, 1125–1156, 2005,

<http://www.atmos-chem-phys.net/5/1125/2005/>. 7219, 7224, 7225, 7230

Textor, C., Schulz, M., Guibert, S., Kinne, S., Balkanski, Y., Bauer, S., Berntsen, T., Berglen, T., Boucher, O., Chin, M., Dentener, F., Diehl, T., Easter, R., Feichter, H., Fillmore, D., Ghan, S., Ginoux, P., Gong, S., Kristjansson, J., Krol, M., Lauer, A., Lamarque, J., Liu, X., Montanaro, V., Myhre, G., Penner, J., Pitari, G., Reddy, S., Seland, O., Stier, P., Takemura, T., and Tie, X.: Analysis and quantification of the diversities of aerosol life cycles within AeroCom, Atmos. Chem. Phys., 6, 1777–1813, 2006,

<http://www.atmos-chem-phys.net/6/1777/2006/>. 7229

Tost, H., Jöckel, P., Kerkweg, A., Sander, R., and Lelieveld, J.: Technical note: A new comprehensive SCAVenging submodel for global atmospheric chemistry modelling, Atmos. Chem. Phys., 6, 565–574, 2006a. 7222, 7226

Tost, H., Jöckel, P., and Lelieveld, J.: Influence of different convection parameterisations in a GCM, Atmos. Chem. Phys., 6, 5475–5493, 2006b. 7222

Tost, H., Jöckel, P., and Lelieveld, J.: Lightning and convection parameterisations – uncertainties in global modelling, Atmos. Chem. Phys., pp. 4553–4568, 2007. 7222

Vehkamäki, H., nad I. Napari, M. K., Lehtinen, K., Timmreck, C., Noppel, M., and Laaksonen, A.: An improved parameterization for sulfuric acid-water nucleation rates for tropospheric and stratospheric conditions, J. Geophys. Res., 107, 4622, doi:10.1029/2002JD002184, 2002. 7225

Vignati, E., Wilson, J., and Stier, P.: M7: An efficient size-resolved aerosol microphysics module for large-scale aerosol transport, J. Geophys. Res., 109, D22202, doi: 10.1029/2003JD004486, 2004. 7224, 7225

von Glasow, R. and Sander, R.: Variation of sea salt aerosol pH with relative humidity, Geophys. Res. Lett., 28, 247–250, 2001. 7219

Wagner, T., Leue, C., Wenig, M., Pfeilsticker, K., and Platt, U.: Spatial and temporal distribution of enhanced boundary layer BrO concentrations measured by GOME instrument onboard ERS-2, J. Geophys. Res., 106, 24 225–24 235, 2001. 7219

Wesely, M.: Parameterization of the surface resistances to gaseous dry deposition in regional-scale numerical models, Atmos. Environ., 23, 1293–1304, 1989. 7226

Wilson, J., Cuvelier, C., and Raes, F.: A modeling study of global mixed aerosol fields, J. Geophys. Res., 106, 34 081–34 108, 2001. 7225

**Part-I: model
description, sea salt
aerosols and pH**

A. Kerkweg et al.

Title Page

Abstract

Introduction

Conclusions

References

Tables

Figures

◀

▶

◀

▶

Back

Close

Full Screen / Esc

Printer-friendly Version

Interactive Discussion



Table 1. List of all abbreviations used in this article.

abbreviation	
AC-GCM	Atmospheric Chemistry General Circulation Model
ACE 1	First Aerosol Characterisation Experiment
ADM	aerosol dynamical model
AEROCE	(aerosol) measurement network
AeroCom	Aerosol Comparison experiment
AIRSEA	MESSy submodel: trace gas air-sea exchange
BC	black carbon (aerosol component, M7)
CLOUD	MESSy submodel: cloud microphysics
CONVECT	MESSy submodel: convection param.
CVTRANS	MESSy submodel: convective transport of tracers
DMS	dimethyl sulphide
DRYDEP	MESSy submodel: dry deposition of gases and aerosols
DU	dust (aerosol component, M7)
E5/M1	ECHAM5/MESSy version1
E5/M1 ⁺	extended ECHAM5/MESSy1 version, used in this study
ECHAM5	GCM (Max-Planck-Institute for Meteorology, Germany)
ECHAM5-HAM	ECHAM5 version including the HAM
ECMWF	European Centre of Medium-range Weather Forecasting
EMEP	(aerosol) measurement network
H2O	MESSy submodel: chemical tendency of H ₂ O and feedback
HAM	Hamburg Aerosol Model (based on the ADM M7 + 3d sources and sinks)
HETCHEM	MESSy submodel: heterogeneous chemistry
IMPROVE	(aerosol) measurement network
JVAL	MESSy submodel: photolysis rates
L87 / L90	abbr. for vertical number of layers (L87 = 87 vertical layers)
LNOX	MESSy submodel: Lightning NO _x
LWC	liquid water content
M7	MESSy submodel: an ADM
MAECHAM5	middle atmosphere version of ECHAM5
MECCA(-AERO)	MESSy submodel: gas and aerosol phase chemistry
MESSy	Modular Earth Submodel System
OC	organic carbon (aerosol component, M7)
ODE	ordinary differential equation
OFFLEM	MESSy submodel: offline emissions
ONLEM	MESSy submodel: online emissions
PDF	Probability Density Functions
PSC	MESSy submodel: polar stratospheric clouds
RAD4ALL	MESSy submodel: radiation
QBO	Quasi-Biennial Oscillation (process and MESSy submodel)
SCAV	MESSy submodel: scavenging and cloud chemistry of gases and aerosol particles
SEDI	MESSy submodel: sedimentation of aerosol particles
SS	sea salt (aerosol component, M7)
SU	sulphate (aerosol component, M7)
TNUDGE	MESSy submodel: tracer nudging
TROPOP	MESSy submodel: tropopause diagnostic

Part-I: model description, sea salt aerosols and pH

A. Kerkweg et al.

Title Page

Abstract

Introduction

Conclusions

References

Tables

Figures

◀

▶

◀

▶

Back

Close

Full Screen / Esc

Printer-friendly Version

Interactive Discussion



Part-I: model description, sea salt aerosols and pH

A. Kerkweg et al.

Table 2. Distribution and characteristics of aerosol components in the M7 modes: SU=sulphate; OC=organic carbon; BC=black carbon; SS=sea salt; DU=dust.

Mode	SU	OC	BC	DU	SS	radius range [μm]
1 nucleation soluble	x					$\bar{r} \leq 0.005$
2 Aitken soluble	x	x	x			$0.005 < \bar{r} \leq 0.05$
3 accumulation soluble	x	x	x	x	x	$0.05 < \bar{r} \leq 0.5$
4 coarse soluble	x	x	x	x	x	$0.5 < \bar{r}$
5 Aitken insoluble		x	x			$0.005 < \bar{r} \leq 0.05$
6 accumulation insoluble				x		$0.05 < \bar{r} \leq 0.5$
7 coarse insoluble				x		$0.5 < \bar{r}$

Title Page

Abstract

Introduction

Conclusions

References

Tables

Figures

◀

▶

◀

▶

Back

Close

Full Screen / Esc

Printer-friendly Version

Interactive Discussion



Part-I: model description, sea salt aerosols and pH

A. Kerkweg et al.

Table 3. Annually averaged primary emissions, dry deposition, sedimentation and wet deposition of M7 components. The units are Tg(S) for SU and Tg(C) for OC and BC, respectively.

component	burden (Tg)	lifetime (days)	primary emission (Tg/yr)	dry deposition (Tg/yr)	sedimentation (Tg/yr)	wet deposition (Tg/yr)
SU	0.4		0.0	0.9	0.8	1.2
OC	1.0	4.1	88.0	6.0	3.6	66.2
BC	0.1	4.7	7.7	0.5	0.3	5.3
DU	5.6	3.7	554.2	34.6	112.3	275.8
SS	7.3	0.5	5213.3	1520.0	829.9	2774.1
Accumulation	0.1	0.6	56.3	3.8	0.1	11.1
Coarse	7.2	0.5	5157.0	1516.2	829.8	2763.0

Title Page

Abstract

Introduction

Conclusions

References

Tables

Figures

◀

▶

◀

▶

Back

Close

Full Screen / Esc

Printer-friendly Version

Interactive Discussion



Part-I: model description, sea salt aerosols and pH

A. Kerkweg et al.

Table 4. List of published coarse mode aerosol pH measurements.

	pH (measured)	location		time	reference
A	3.5–4.5	Bermuda,	32°N, 64°W	April–May 1996	Keene and Savoie (1999)
B	2–5	Southern ocean,	40°–55°S, 60°–135°E	18.11.–11.12.1995	Fridlind and Jacobson (2000)
C	3.3–5.3	Bermuda,	32°N, 64°W	2–27 May 1997	Keene et al. (2002)
D	4.5–5.4	Hawaii,	21°N, 157°W	4–29 September 1999	Pszenny et al. (2004)
E	1.9–3.3	US east coast		July/August 2002	Keene et al. (2004)

Title Page

Abstract

Introduction

Conclusions

References

Tables

Figures

◀

▶

◀

▶

Back

Close

Full Screen / Esc

Printer-friendly Version

Interactive Discussion



**Part-I: model
description, sea salt
aerosols and pH**

A. Kerkweg et al.

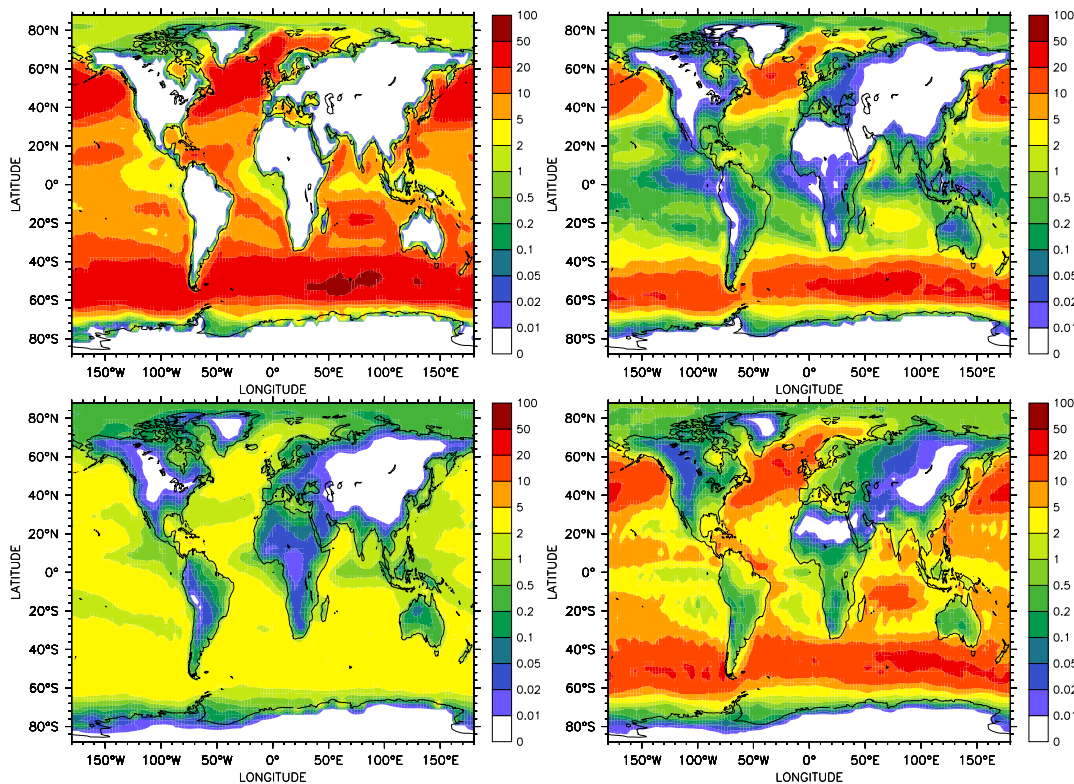


Fig. 1. Annually averaged sea salt sources and sinks (g/(m²yr)): top left: emission; top right: dry deposition; bottom left: sedimentation and bottom right: wet deposition.

[Title Page](#)[Abstract](#)[Introduction](#)[Conclusions](#)[References](#)[Tables](#)[Figures](#)[◀](#)[▶](#)[◀](#)[▶](#)[Back](#)[Close](#)[Full Screen / Esc](#)[Printer-friendly Version](#)[Interactive Discussion](#)

**Part-I: model
description, sea salt
aerosols and pH**

A. Kerkweg et al.

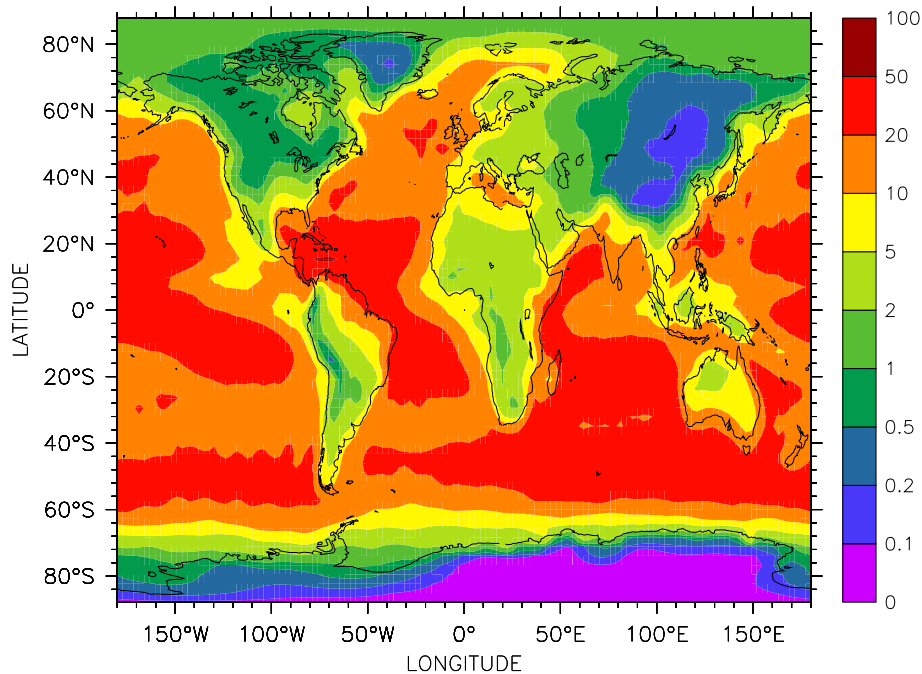


Fig. 2. Annually averaged vertically integrated atmospheric sea salt column mass (mg/m^2).

[Title Page](#)[Abstract](#)[Introduction](#)[Conclusions](#)[References](#)[Tables](#)[Figures](#)[◀](#)[▶](#)[◀](#)[▶](#)[Back](#)[Close](#)[Full Screen / Esc](#)[Printer-friendly Version](#)[Interactive Discussion](#)

**Part-I: model
description, sea salt
aerosols and pH**

A. Kerkweg et al.

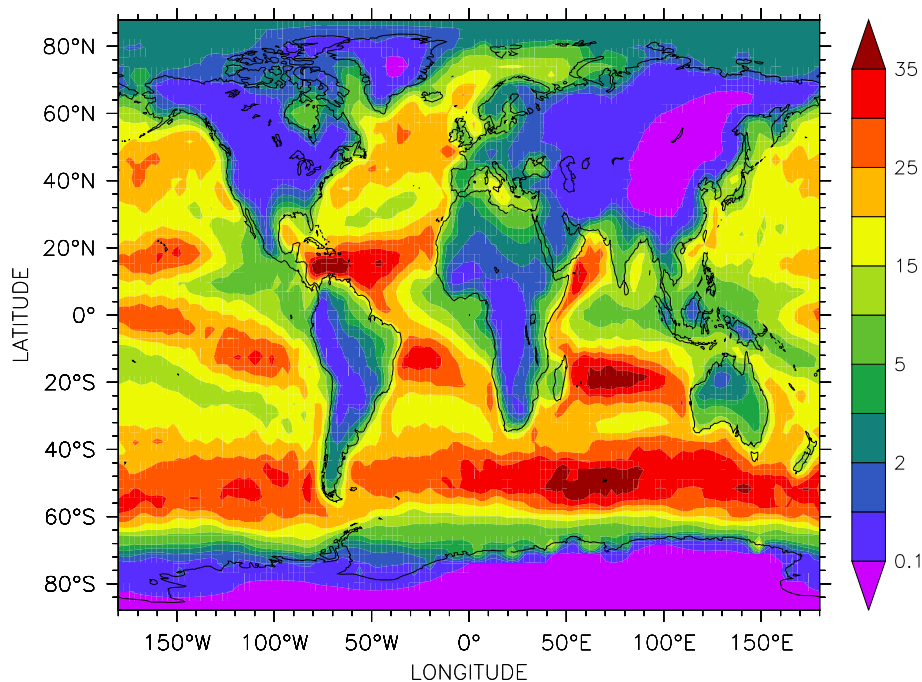


Fig. 3. Annually averaged (coarse mode) sea salt aerosol concentration ($\mu\text{g}/\text{m}^3$) in the lowest model layer.

[Title Page](#)[Abstract](#)[Introduction](#)[Conclusions](#)[References](#)[Tables](#)[Figures](#)[◀](#)[▶](#)[◀](#)[▶](#)[Back](#)[Close](#)[Full Screen / Esc](#)[Printer-friendly Version](#)[Interactive Discussion](#)

Part-I: model description, sea salt aerosols and pH

A. Kerkweg et al.

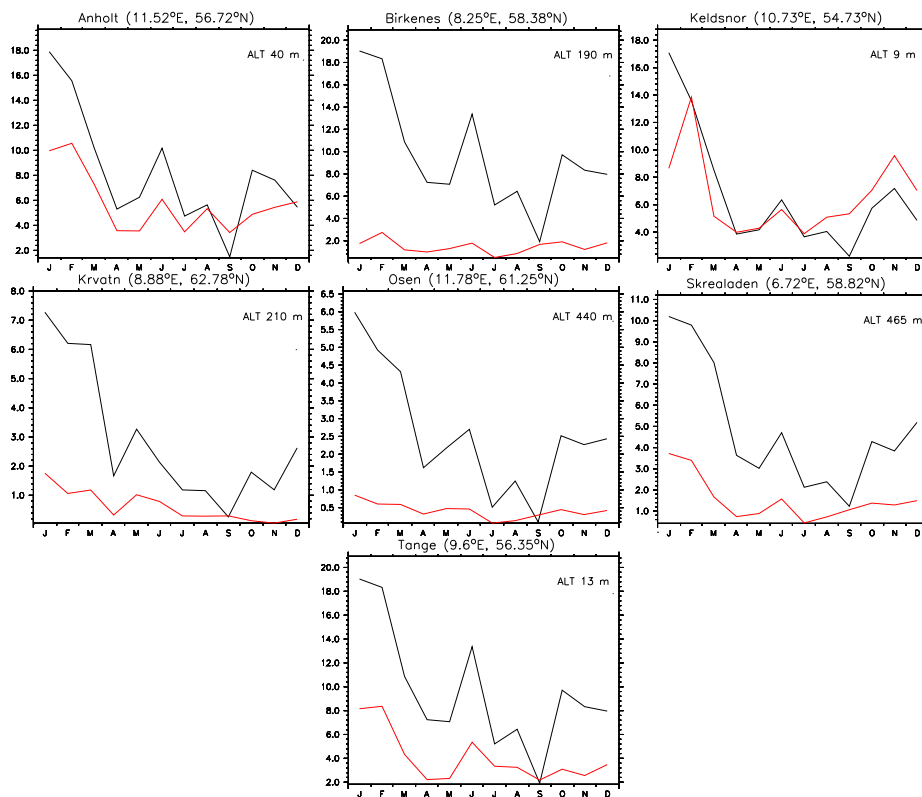


Fig. 4. Comparison of sea salt concentrations ($\mu\text{g}/\text{m}^3$) measured from the EMEP network (red) with the simulated concentrations (black). The stations are in alphabetic order.

Title Page

Abstract

Introduction

Conclusions

References

Tables

Figures

◀

▶

◀

▶

Back

Close

Full Screen / Esc

Printer-friendly Version

Interactive Discussion



Part-I: model description, sea salt aerosols and pH

A. Kerkweg et al.

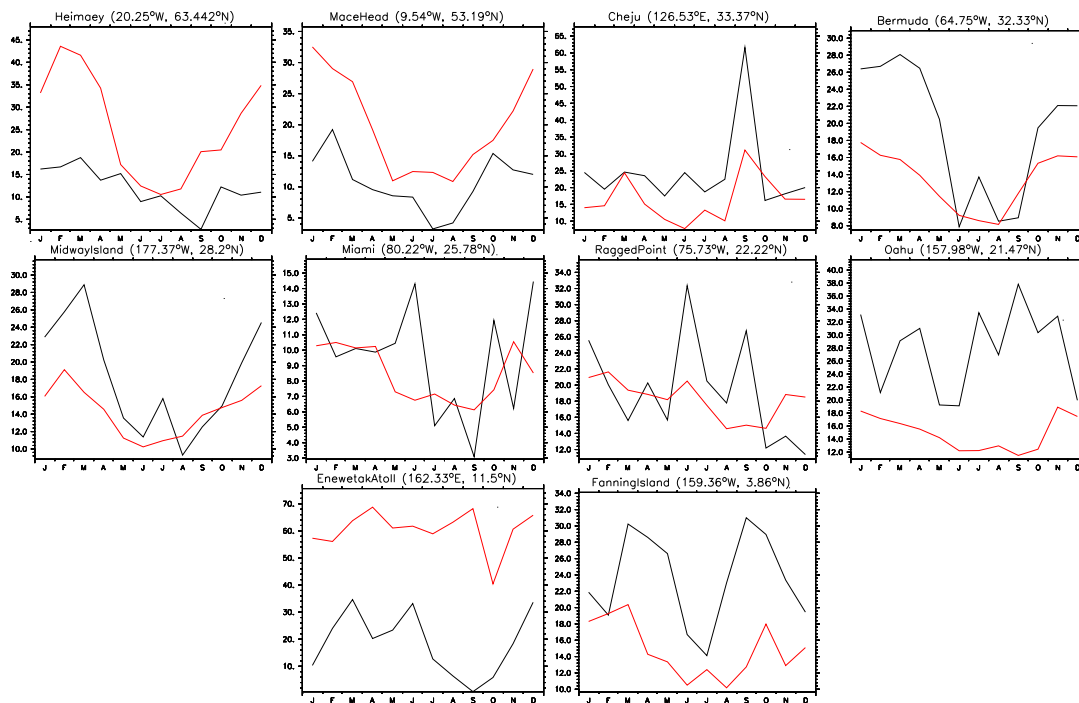


Fig. 5. As Fig. 4 for AEROCE (red). The stations are sorted from north to south.

Title Page

Abstract

Introduction

Conclusions

References

Tables

Figures

◀

▶

◀

▶

Back

Close

Full Screen / Esc

Printer-friendly Version

Interactive Discussion



Part-I: model description, sea salt aerosols and pH

A. Kerkweg et al.

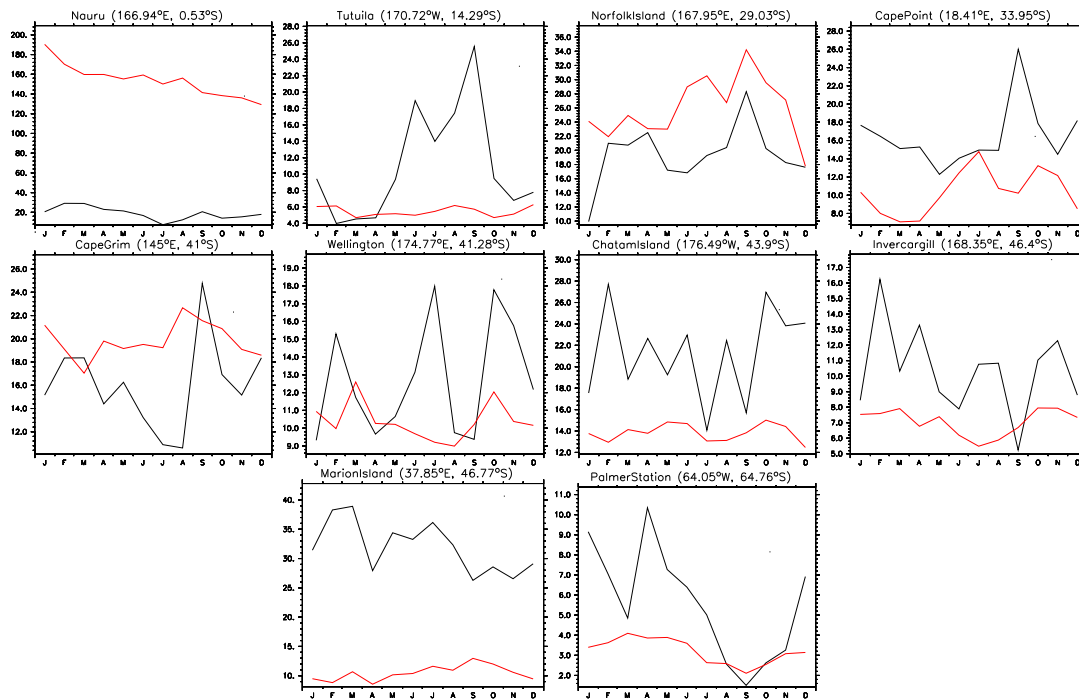


Fig. 5. Continued.

Title Page

Abstract

Introduction

Conclusions

References

Tables

Figures

◀

▶

◀

▶

Back

Close

Full Screen / Esc

Printer-friendly Version

Interactive Discussion



**Part-I: model
description, sea salt
aerosols and pH**

A. Kerkweg et al.

Title Page

Abstract

Introduction

Conclusions

References

Tables

Figures

◀

▶

◀

▶

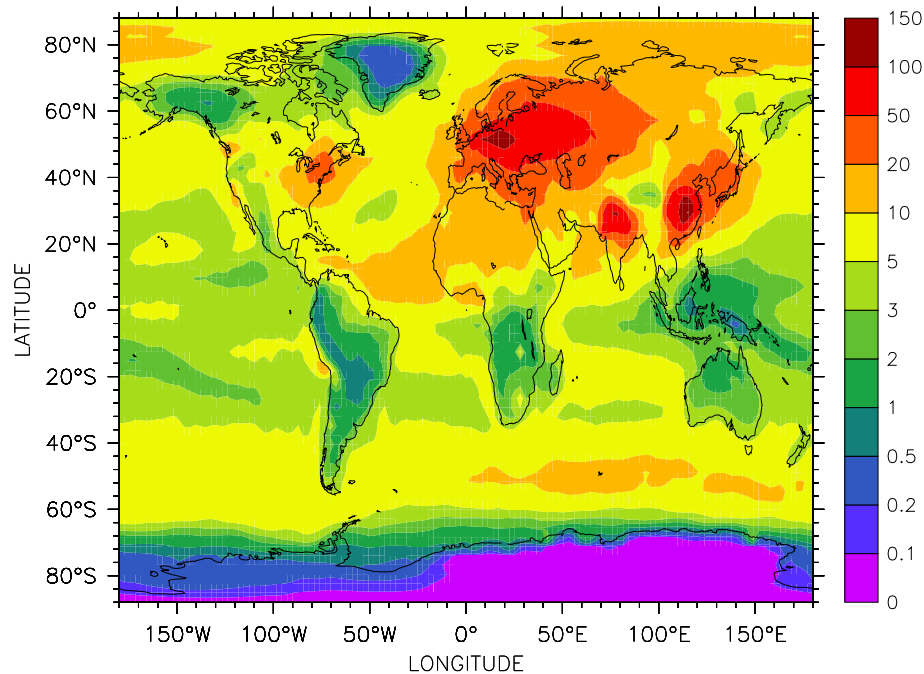
Back

Close

Full Screen / Esc

Printer-friendly Version

Interactive Discussion

**Fig. 6.** Annually averaged coarse mode particle concentration (cm^{-3}) in the lowest model layer.

**Part-I: model
description, sea salt
aerosols and pH**

A. Kerkweg et al.

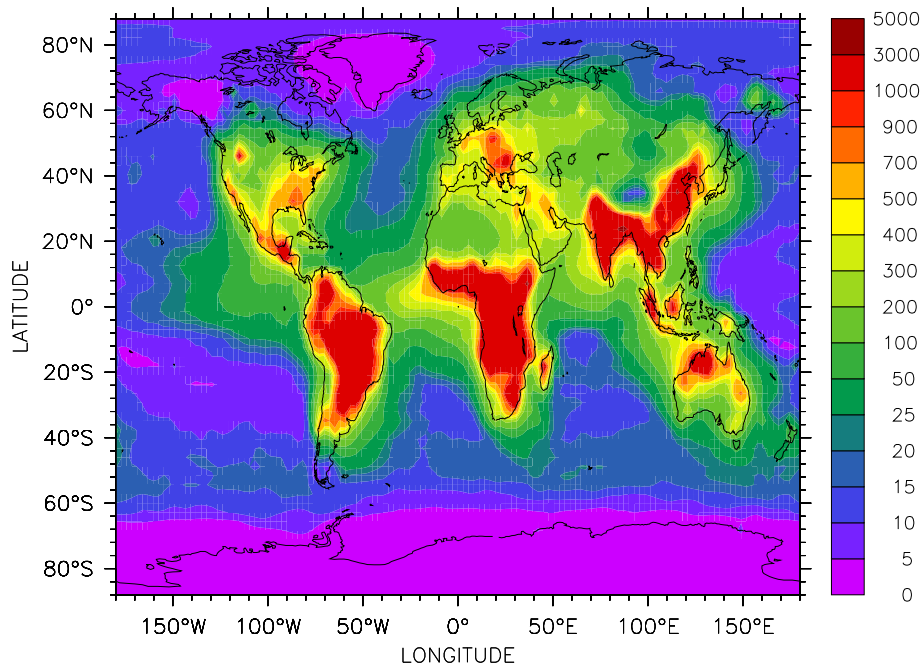


Fig. 7. Annually averaged accumulation and coarse mode particle concentration (cm^{-3}) in the lowest model layer.

[Title Page](#)[Abstract](#)[Introduction](#)[Conclusions](#)[References](#)[Tables](#)[Figures](#)[◀](#)[▶](#)[◀](#)[▶](#)[Back](#)[Close](#)[Full Screen / Esc](#)[Printer-friendly Version](#)[Interactive Discussion](#)

**Part-I: model
description, sea salt
aerosols and pH**

A. Kerkweg et al.

Title Page

Abstract

Introduction

Conclusions

References

Tables

Figures

◀

▶

◀

▶

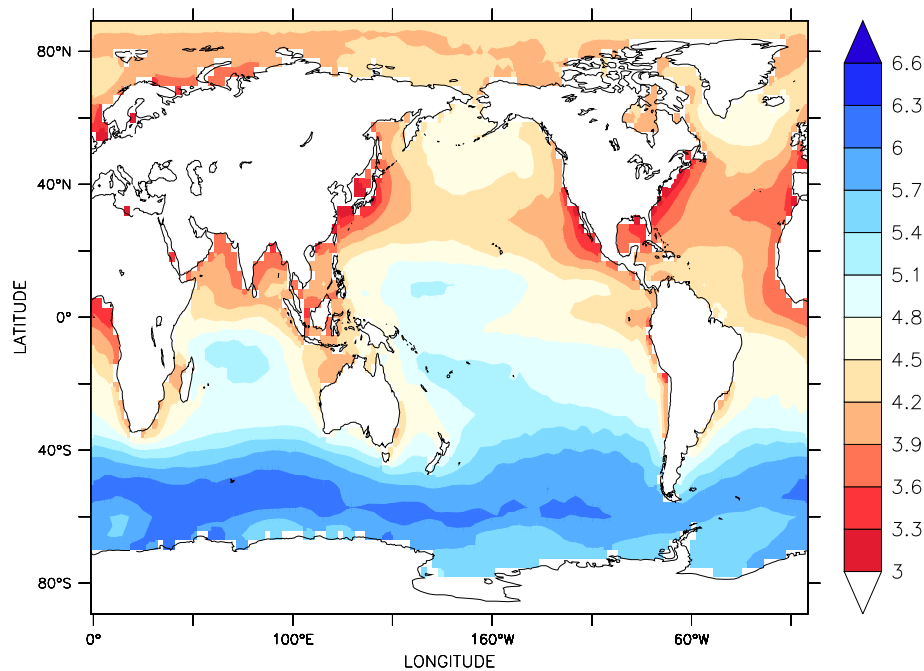
Back

Close

Full Screen / Esc

Printer-friendly Version

Interactive Discussion

**Fig. 8.** Annually averaged boundary layer coarse mode aerosol pH for the year 2000.

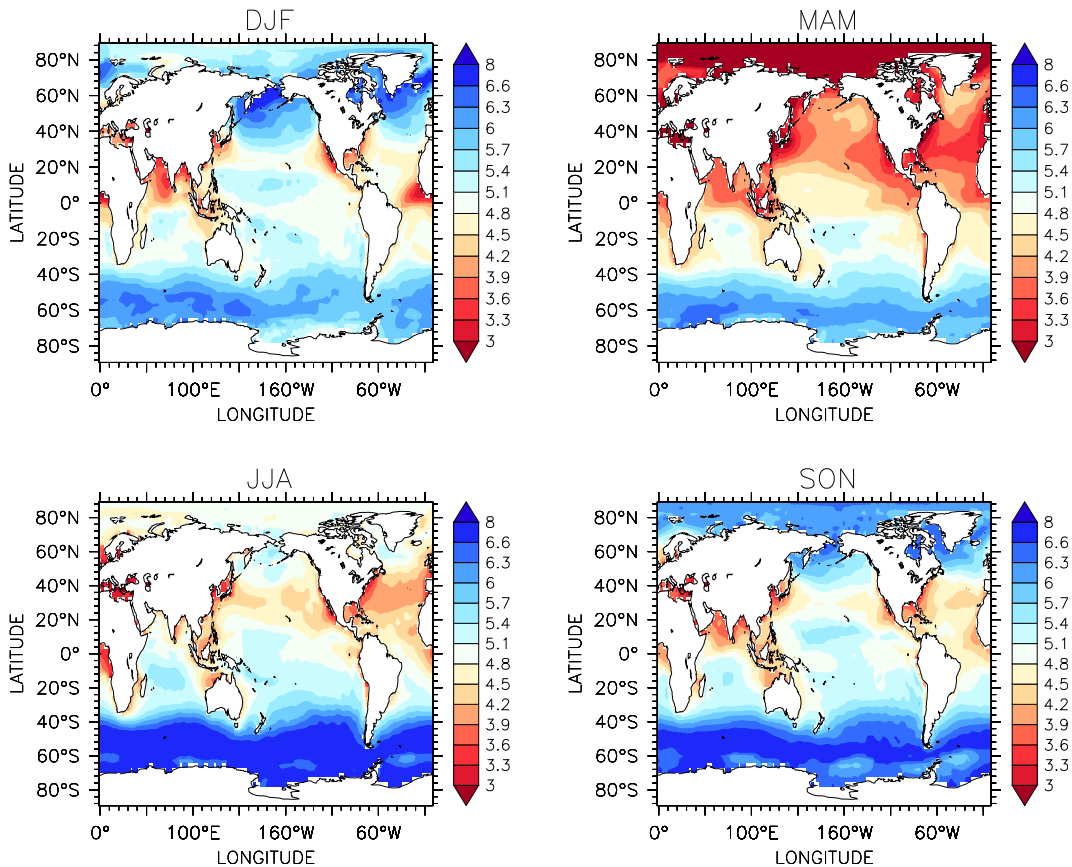


Fig. 9. Seasonally averaged boundary layer sea salt aerosol pH. (DJF: December, January, February; MAM: March, April, May; JJA: June, July, August; SON: September, October, November).

Part-I: model description, sea salt aerosols and pH

A. Kerkweg et al.

Title Page

Abstract

Introduction

Conclusions

References

Tables

Figures



Back

Close

Full Screen / Esc

Printer-friendly Version

Interactive Discussion



**Part-I: model
description, sea salt
aerosols and pH**

A. Kerkweg et al.

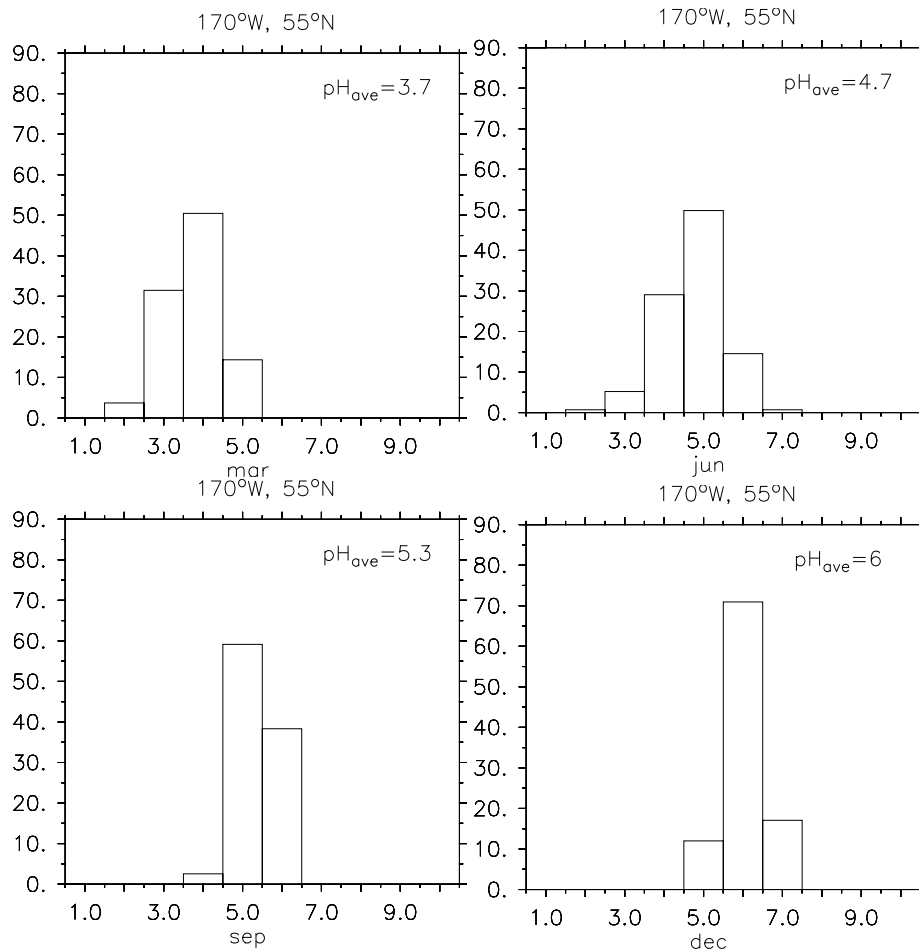


Fig. 10. Probability density functions (PDF, normalised to 100%) of simulated boundary layer pH values at 170°W, 55°N for March, June, September and December of the year 2000.

[Title Page](#)[Abstract](#)[Introduction](#)[Conclusions](#)[References](#)[Tables](#)[Figures](#)[◀](#)[▶](#)[◀](#)[▶](#)[Back](#)[Close](#)[Full Screen / Esc](#)[Printer-friendly Version](#)[Interactive Discussion](#)

**Part-I: model
description, sea salt
aerosols and pH**

A. Kerkweg et al.

Title Page

Abstract

Introduction

Conclusions

References

Tables

Figures

◀

▶

◀

▶

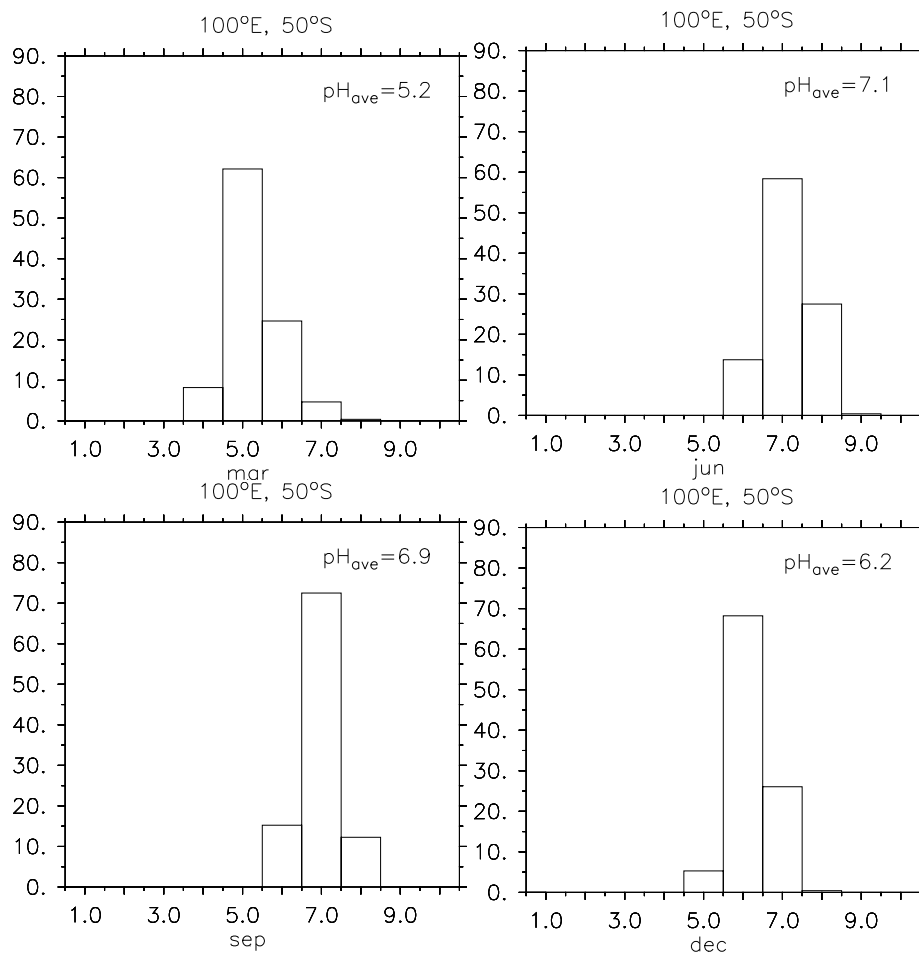
Back

Close

Full Screen / Esc

Printer-friendly Version

Interactive Discussion

**Fig. 11.** As Fig. 10: PDFs of simulated boundary layer pH values at 100°E, 50°S.

**Part-I: model
description, sea salt
aerosols and pH**

A. Kerkweg et al.

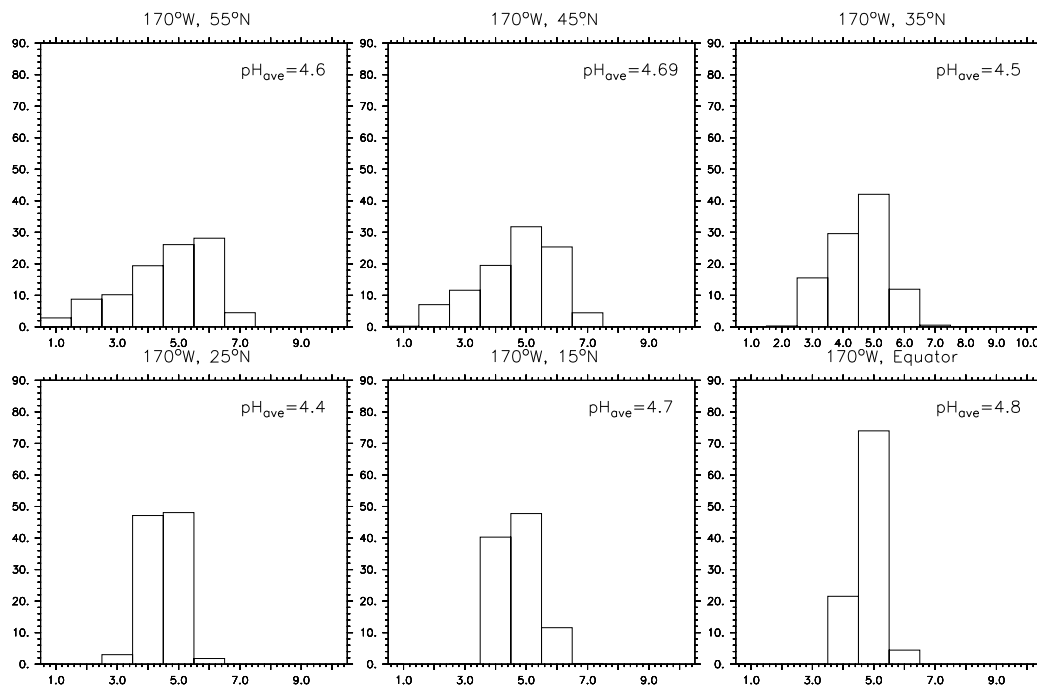


Fig. 12. PDFs of simulated boundary layer pH values at 6 locations in the Pacific at the same longitude.

[Title Page](#)[Abstract](#)[Introduction](#)[Conclusions](#)[References](#)[Tables](#)[Figures](#)[◀](#)[▶](#)[◀](#)[▶](#)[Back](#)[Close](#)[Full Screen / Esc](#)[Printer-friendly Version](#)[Interactive Discussion](#)

**Part-I: model
description, sea salt
aerosols and pH**

A. Kerkweg et al.

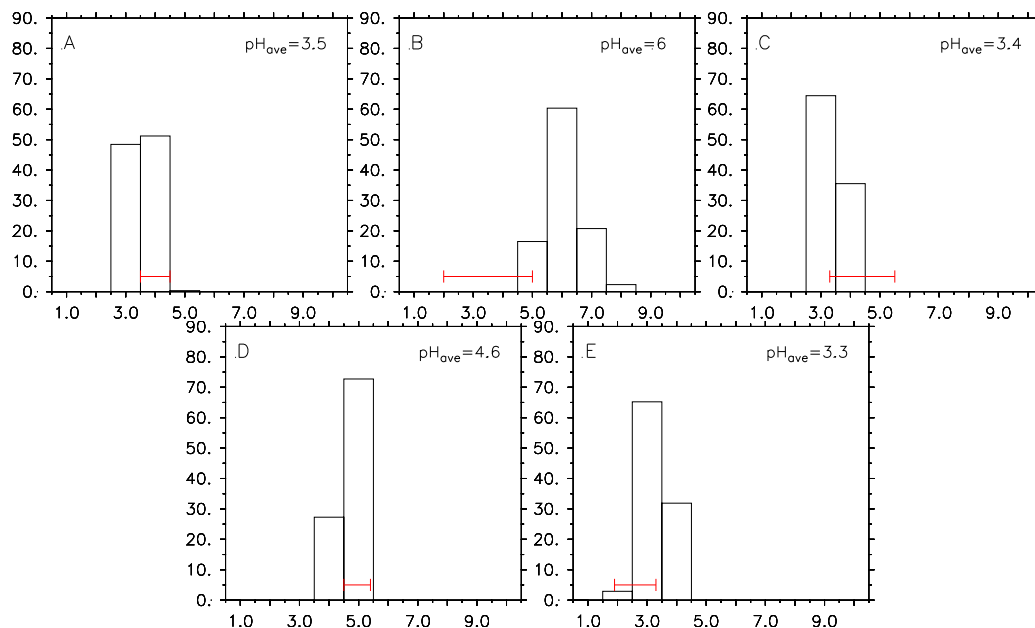


Fig. 13. Measured coarse mode aerosol pH and simulated probability density functions (PDFs) of pH values at locations and times of measurements listed in the Table 4. The red bars indicate the ranges of the measurements. The letters A–E refer to the measurements listed in Table 4.

Title Page

Abstract

Introduction

Conclusions

References

Tables

Figures

◀

▶

◀

▶

Back

Close

Full Screen / Esc

Printer-friendly Version

Interactive Discussion

